Femtosecond Lasers for Quantum Information Technology

Regina de Vivie-Riedle* and Ulrike Troppmann

Department Chemie, Ludwig Maximilians Universität, Butenandtstrasse 11, 81377 München, Germany

Received July 13, 2006

Contents

Regina de Vivie-Riedle was born April 18, 1958, in Wuppertal, Germany. She graduated in Theoretical Chemistry from the Friedrich-Wilhelm-University of Bonn in 1987. She worked as a postdoc at the MPI for Quantum Optics in Garching and at JILA in Boulder. In 1997 she did her Habilitation in Theoretical Chemistry at the FU Berlin. From 1997 to 2002 she was a C3 professor at the MPI for Quantum Optics. Since 2003 she has been leading the theoretical femtoscience group at the Chemistry Department of the LMU in Munich. Her research topics are femtoscience, coherent control theory, molecular quantum computing, and cold molecules

Ulrike Troppmann was born July 13, 1977, in Munich, Germany. She graduated in chemistry from the Ludwig-Maximilians-University of Munich in 2002 and obtained her Ph.D. in physical chemistry there in 2006. During her diploma and also her Ph.D. work, she conducted theoretical studies on the application of ultrashort and specially shaped laser pulses in the IR regime for quantum computation with qubits encoded in molecular vibrations. Her main research interests also include optimal control theory and the coherent control of intramolecular vibrational energy transfer.

1. Introduction

The technological needs imposed by the exponential miniaturization trend of electronic components has drawn attention toward the development of functional molecular or even atomic devices. Quantum effects become increasingly dominant on the atomic length scale, and precise control of quantum systems arises as a fundamental requirement for successful novel nanoscale technology. Promising results have already been achieved in the fields of molecular electronics,[1] data storage,[2] and quantum information processing.[3] Pioneered by the molecular physics community, optimal control[4−7] has emerged as a highly promising tool. Strengthened by successful control experiments on chemical reactions[8−11] and biological processes,[12] it has also entered the fields of quantum optics,[13] solid-state physics,[14] and nuclear magnetic resonance (NMR).[15]

From the computing point of view, the continuous downsizing of microprocessor components as well as the desire for a further increase of calculation speed are accompanied by the need for a new quantum technology, which has to be established in the near future. It turns out that, besides a computational speed up, quantum technology leads to a completely new kind of computation: new concepts and algorithms complete or replace the common classical methods.[16] Prominent quantum algorithms are the Deutsch Jozsa,[17] the Shor,[18] and the Grovers search algorithms.[19] The information is coded in quantum bits (qubits), each one represented by two selected and preferably well isolated quantum states. In contrast to classical computing, it is possible to

10.1021/cr040094l CCC: $65.00
Published on Web 10/23/2007

generate the respective superposition states and use them. To implement logic operations, that is, quantum gates, tunable interactions between the qubit states are needed. The interaction between different qubits becomes essential for conditional quantum gates, where the operation on one qubit depends on the value of another qubit. As in classical computing, there exist special sets of elementary logic operations from which every desired algorithm can be constructed. The requirements for the construction of a useful quantum computer have been established partly by Deutsch[17] and completed by DiVincenzo.[20] These also include scalability of the system, readout methods, and error correction.

Especially in this rapidly expanding field of quantum information processing, the controllability of quantum systems is a key issue. The search for the ideal qubit system as well as the most applicable control technologies is still open, and proposals range from photons and atoms to molecules and semiconductors driven by specially adapted electromagnetic fields. Considerable success in quantum information processing was achieved for a limited number of qubits using cavity quantum electrodynamics,[21] trapped ions,[22,23] and NMR.[24−26] Approaches with atoms, ions, and quantum dots use electron degrees of freedom to encode quantum information in well isolated, identical qubits with equal transition frequencies. The interqubit interaction can be turned on or off on demand. Enlarging these qubit systems from two-qubit to multiqubit systems means, in principle, that another atom, ion, or quantum dot has to be added. Liquid NMR quantum computing makes use of nuclear spin in molecules as the carrier of quantum information and differs from the previous approaches in some aspects. Each qubit is still encoded in a well isolated two-level spin system, but in response to the internal molecular environment, the transition frequencies of the qubits can differ. Also, the interaction between qubits is already an inherent molecular property. Enlargement of the qubit system in NMR involves more atoms of a molecule and is supported by molecular engineering.

The most promising and advanced experiments with respect to the realization of entanglement, quantum gates, and quantum algorithms were demonstrated with NMR and ion traps. In NMR, the Shor algorithm with up to seven nuclear spin qubits could be implemented,[27] and in ion traps, entanglement with up to eight particles has been reported.[28] While these first examples demonstrate that enlargement of qubit systems is in principle possible, real scalability remains a challenge in all approaches. Scalability, in general, requires that the effort and overhead associated with making and controlling multiqubit systems scale only polynomially with the number of qubits. Although for some approaches, for example, quantum dots or electron spins in solid state systems, the setup of large scale multiqubit systems seems straightforward, their precise control is still an open question. Especially for the ion trap approach, some promising ideas to realize scalability have been put forth. In this context, either a "hybrid" ansatz is favored with ions stored in individual traps and a quantum channel established in between them for information exchange[29] or an ion trap network is favored with small qubit entities being processed and transported between different interaction regions.[30] No single technology under investigation currently meets all requirements to implement a quantum computer in a completely satisfactory way. Therefore, ongoing research in quantum information processing is highly interdisciplinary and diverse and requires a coordinated effort to create synergies. In this review, we focus on recent developments in a new direction of quantum information processing using internal molecular degrees of freedom as qubits. It has been realized by several groups working in the field of coherent control with femtosecond laser pulses that certain control sequences can be interpreted as quantum logic operations or even quantum algorithms. Different from NMR quantum computing, which uses the nuclear spin of atoms, this new approach works with internal motional states of molecules such as rovibrational states[31] and vibrational states in diatomic[32−35] and polyatomic systems.[36−40] The relevant time scale for the internal mode qubits is in the femtosecond regime, and their dynamics can be controlled by modulated femtosecond laser pulses. Our aim is to elucidate the connection between coherent control with modulated femtosecond laser fields and quantum computing with molecular degrees of freedom. Molecules instead of atoms or ions provide a number of properties that can be useful in the context of quantum computing. They are small, stable units with a rich quantum structure due to many coupled degrees of freedom. With the help of chemists, a nearly unlimited number of compounds offering all kinds of properties can be designed. In the context of quantum computing, in addition to long coherence lifetimes, characteristic optical and spectral properties are aimed for.

In this review, we select the molecular vibrational quantum computing ansatz as a representative example for modulated femtosecond laser pulses in quantum information science. We approach this issue from the theory side, taking into account the experimental requirements of state-of-the-art pulse shaping technology. Specific challenges and advantages for the molecular approach as well as realistic implementation strategies are outlined. The setup of the qubit system is explained in section 2. In section 3, we discuss both the sides of quantum control and of quantum computing with the main focus on polyatomic molecules as qubit systems. Mechanistic aspects of quantum gates and issues of phase coherence as well as the choice of suitable molecules are discussed in section 4, and section 5 deals with implementations of complete quantum algorithms. Section 6 addresses experimental realization strategies of the control laser fields. The open issues of decoherence control and scalability will be discussed in section 7. In section 8, we give a general conclusion and an outlook for the impact of femtosecond laser technology in the field of quantum computing.

2. Qubit Systems and Logic Operations

In the following, we briefly introduce the general ideas of quantum computing and translate them into the molecular approach we will focus on. We present the theoretical description of the molecular quantum system as well as the control Hamiltonian. The system Hamiltonian determines the eigenfunctions and eigenenergies, including possible potential or kinetic couplings. The qubits are encoded in selected eigenfunctions and are embedded in the vibrational spectrum. The control Hamiltonian, exploited to perform the desired quantum gates, arises from the application of specially modulated femtosecond laser fields in the IR, mid-IR, or UV/vis regime.

The main differences between classical and quantum computing result from the definition of the basic unit of information: the bit. From a physical point of view, a bit is a two-state system. It can be represented using two logical

values: 0 and 1. In a classical computer, these values can be coded through voltage or no voltage in an electric circuit. Bits of information can also be coded in a quantum system, and are then accordingly called quantum bits or qubits. Here, special states of a quantum system, which can be switched by the action of, for example, an electromagnetic field, are selected to encode the logical values $|0\rangle$ and $|1\rangle$. For example, different degrees of electronic excitation in atoms or different orientations of spins can be used. In contrast to the classical case, quantum bits can also be in a coherent superposition state:

$$|\psi\rangle = \alpha|0\rangle + \beta|1\rangle; \quad |\alpha|^2 + |\beta|^2 = 1; \quad \alpha,\beta \in \mathbb{C} \quad (1)$$

In principle, an infinite number of possible states $|\psi\rangle$ exists even for a single qubit. Since the superposition states cannot be distinguished by a single measurement, only evenly distributed superposition states ($|\alpha|^2 = |\beta|^2 = 0.5$) are used in quantum information processing. Classically, *n* bits can form only a $2n$ dimensional state space. In contrast, *n* qubits span a 2^n dimensional Hilbert space. The logic operations in the qubit system are performed by so-called quantum gates. In his catalog of requirements, DiVincenzo demands for a universal set of elementary quantum gates. Mathematically, these quantum gates are time reversible unitary transformations. Experimentally, they can be realized by applying appropriate electric or magnetic fields. Running through a quantum algorithm, one has the possibility to simultaneously code several states and their evolution in (evolving) superposition states. This fact is called quantum parallelism. It is one of the main reasons for the high efficiency of quantum algorithms. Still, during the readout of the state of a qubit, the corresponding wave function collapses into one of its basis states, and the value 0 or 1 can be measured with a certain probability. Therefore, quantum algorithms work somewhat differently from classical algorithms: The probability to measure the result of interest is increased. Another important feature of quantum information systems is the phenomenon of quantum correlation or entanglement. It can be found in multiqubit states. The results of measurements conducted on entangled qubits are highly correlated, although the measurement outcome of an individual qubit is still purely statistic. The well-known Bell and GHZ (Greenberger, Horne, Zeilinger) states belong to this category.[41] The coherence of superposition states or entangled states plays an important role in several quantum algorithms, for example, the Shor algorithm.

In summary, the coherence of multiqubit systems is the source of useful quantum information and has to be maintained as long as possible in the qubit system. In practice, the physical system constituting the quantum computer and the quantum gating devices are never completely isolated from their environment, which acts as a heat bath or reservoir. The density operator describing the state of the quantum computer does not remain pure (nonunitary evolution), as it can be changed by the intersystem or system-environment interactions into a mixed state. Simultaneously, the initially prepared coherences between the input states will be partially or completely destroyed. This process of decoherence is destructive for quantum computation; therefore, ideally the decoherence time scale should be much longer than the gating time scales. From analytic methods such as spectroscopy or spectrometry, a lot of knowledge has been accumulated concerning internal quantum states of atoms, molecules, and bigger aggregates up to solids, their manipulation, and the corresponding issues of coherence and decoherence. Naturally, first quantum computing approaches have been developed based on these methods and this knowledge.[24,29]

2.1. Molecular Qubits

Molecules are highly complex quantum systems with many coupled degrees of freedom, including electronic as well as nuclear motion, that offer a variety of properties. Accordingly, several choices can be made to encode a qubit system in molecules. Besides nuclear spin (NMR), rovibrational wave packets or vibrational states were tested. In molecular systems, sources of decoherence are the coupling to internal molecular modes outside the Hilbert space of the qubit basis and the coupling to the environment by collision with other molecules. Both sources can be suppressed efficiently in case of NMR and vibrational qubits,[37] and the ratio of coherence time to gating time is $\sim 10^3 - 10^4$. The definition of rotational or vibrational eigenstates as qubit states is similar to liquid NMR qubits; however, the quantum logic operations are performed on a different time scale (femtoseconds to picoseconds instead of milliseconds to minutes).

The obvious choice to drive electronic or vibrational molecular quantum states in a controlled way is the application of laser light. Figure 1 schematically visualizes three-qubit and quantum gate implementations, which have been discussed in the literature. IR and Raman processes are thinkable[32,37] to control vibrational modes in the ground state as well as to control rovibrational wave packets in electronic excited states[31,34] by UV/vis lasers. Figure 1a shows the pump−probe approach suggested by Vala et al.[31] After the preparation of a pure input state with a CW (continuous wave) laser, a specially phase modulated femtosecond laser pulse implements the quantum logic. With a final probe pulse, an ionization signal (readout) is produced. Figure 1b shows the CARS sequence as proposed by Zadoyan et al. and Bihary et al.[32,33] for molecular quantum computing. A superposition of rovibrational states is prepared by the first femtosecond pulse, followed by the second shaped femtosecond pulse, which encodes the quantum algorithm and projects the result onto the ground state. From there, the readout is initiated by a third delayed pulse. Figure 1c visualizes the approach, developed in our group,[37] using vibrational normal modes of a polyatomic system to encode individual qubits. The quantum gates in such a multidimensional system can be realized by shaped femtosecond pulses in the IR regime. Preparation and readout can be achieved spectroscopically. A first successful experiment demonstrated the implementation of the Deutsch−Jozsa algorithm with the scheme of Figure 1a.[31] In the following, we will focus on qubits encoded in vibrational modes of polyatomic systems.

2.1.1. Vibrational Qubits

In an *N*-atomic molecule, $3N - 5$ or $3N - 6$ different normal modes can be identified and allocated in the spectroscopic notation ($q_1q_2...q_{3N-6}$), with q_i the number of vibrational quanta in the *i*th normal mode. Depending on the spectroscopic method applied, the respective optically addressable modes can be used to encode qubits. For example, the IR active modes of acetylene (C_2H_2), the *cis*-bending mode, and the asymmetric CH-stretching mode can be selected as qubit modes. In this case, all IR inactive vibrations, such as the *trans*-bending mode in acetylene, are nonqubit modes. Excitations of two different quanta in each

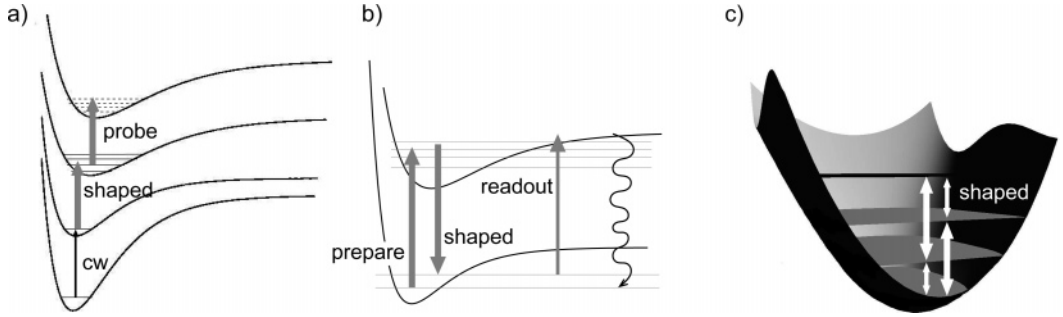

Figure 1. Schematic representation of different molecular qubit systems and quantum logic implementations: (a) VIS−fs−pump−probe sequence with initial state preparation by a CW laser,[16] with the shaped pump laser pulse encoding the quantum logic; (b) TFRCARS implementation of a precompiled algorithm;[18] (c) quantum logic implementation with modulated IR pulses operating on vibrational qubits in the ground state.[22]

qubit mode are referred to as $|0\rangle$ and $|1\rangle$. For the general qubit definition, q quanta of excitation are labeled as logical 0, while $q + 1$ quanta of excitation are labeled as logical 1. One possible qubit definition is to start with zero quanta of excitation in each vibrational mode. In this case, the complete 2^2 dimensional qubit basis of a two-qubit system encoded in a $3N - 6$ normal mode system reads as follows:

$$\begin{aligned}(00\mathbf{0}0...\mathbf{0}) &\equiv |00\rangle\\ (00\mathbf{1}0...\mathbf{0}) &\equiv |10\rangle\\ (00\mathbf{0}0...\mathbf{1}) &\equiv |01\rangle\\ (00\mathbf{1}0...\mathbf{1}) &\equiv |11\rangle\end{aligned} \tag{2}$$

In this example, the third and the last vibrational mode are used to encode the qubits.

Each normal mode vibrates at its own eigenfrequency, and the selected qubit states are embedded in a vibrational spectrum with increasing density for higher quantum numbers. In principle, operations for different qubits can be driven by the specific normal mode eigenfrequencies. However, in almost all molecules, those modes deviate from the ideal normal mode behavior. They are, rather, coupled degrees of freedom, and thus, the transition frequencies for switching, for example, the states $|00\rangle \leftrightarrow |01\rangle$ and $|10\rangle \leftrightarrow |11\rangle$, differ. This qubit−qubit interaction is system inherent and mediated via the molecular bonds. To elucidate the situation, the spectrum of the vibrational states for a two-dimensional (2D) acetylene model is shown in Figure 2. The 2D model is reduced to the two IR active modes, the asymmetric CH-stretch and the *cis*-bending mode, which are selected to encode two qubits. Thus, the qubit system also includes a combination mode, (11). The corresponding 2D wave functions of the qubit basis states $|00\rangle$, $|01\rangle$, $|10\rangle$, and $|11\rangle$ are displayed in the middle of Figure 2. Also shown is the energy spectrum when the 2D acetylene model is augmented by the passive *trans*-bending mode (3D). Now the situation arises that a combination state of the passive mode and the *cis*-bending mode, denoted $|11\rangle$*, is in close resonance to the qubit state $|11\rangle$. The described scenario is a typical molecular property and has to be controlled when quantum logic operations are implemented. This requires highly flexible laser fields that are provided, for example, by shaped femtosecond laser pulses.

To achieve long decoherence times, we have proposed to use low lying vibrational modes of polyatomic systems as qubit states in the IR regime. Thus, the qubit system is close to the molecular ground state and in the less dense spectral region, where the coupling to the molecular surroundings

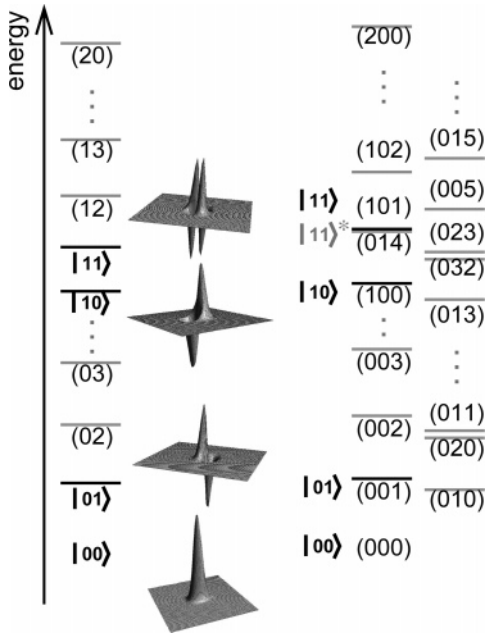

Figure 2. Vibrational spectrum of the 2D (left) and 3D (right) acetylene model; the notation corresponds to the number of vibrational quanta. In the 3D model, the second mode is a nonqubit mode. Qubit basis states are displayed in black, and overtones and combination modes outside the qubit basis in gray. The 2D wave functions corresponding to the basis states are shown in the middle.

as well as to the other vibrational modes is kept low. This leads to comparatively long lifetimes in the nanosecond regime. The freedom of choice for the qubit basis helps to find an almost decoherence-free subspace (on the gating time scale) within the vibrational manifold by avoiding extensive coupling to other normal modes.

2.1.2. Setup of the Hamiltonian

For the development of a specific molecular quantum computing scheme, a theoretical description of the qubit system and the gate operations is needed. To illustrate the potential of modulated femtosecond laser pulses as key elements in quantum information processing, the setup of the selected vibrational quantum information system is outlined. The total Hamiltonian $H_{tot} = H_{sys} + H_{control}$ consists of the system Hamiltonian H_{sys} and the control Hamiltonian $H_{control}$. The latter describes the laser−molecule interaction which realizes the quantum logic operations. The system Hamiltonian can be represented either in coordinate space or in the basis of the system Hamiltonian eigenstates. In coordinate space, the potential energy surface (PES) of the

molecular system, the (transition) dipole moments, necessary for the description of the laser−molecule interaction, and the nuclear wave function are mapped on a grid. The PES contains all relevant information about the intramolecular forces, including anharmonicity and anharmonic coupling. It can be obtained from *ab initio* calculations using a standard quantum chemical package or from parametrized model systems relying on ab initio or spectroscopic data. The qubit states are stationary vibrational eigenstates and are obtained by solving the time independent nuclear Schrödinger equation on the corresponding multidimensional discretized PES. When we perform these calculations on a grid applying a relaxation method,[42] typically up to 200 eigenfunctions are calculated. The laser−molecule interaction requires the solution of the time dependent Schrödinger equation

$$\Psi(t) = U(t)\,\Psi(t=0) = \mathrm{e}^{-iH_{\mathrm{tot}}t}\Psi(t=0) \qquad (3)$$

in the respective representation. Established grid propagation methods and approximations for the time evolution operator $U(t)$ are discussed in ref 43. As every vibrational qubit system is embedded in the total vibrational spectrum, wave packet propagations and laser pulse optimizations have to take into account all the relevant vibrational states. This allows us to describe in detail the vibrational excitation process, including intermediate excitation of overtones and combination bands.

The transition from the grid method to the eigenstate (φ_i) representation is performed by evaluation of the total Hamiltonian matrix elements $\langle\varphi_i|H_{\mathrm{sys}}|\varphi_i\rangle$ and $\langle\varphi_i|H_{\mathrm{control}}|\varphi_j\rangle$ on the grid. Alternatively, the level system can be set up directly from spectroscopic data. The eigenstate basis includes all system inherent potential and kinetic couplings in H_{sys}; the coupling to the laser field is taken into account during the propagation by H_{control}. For the propagator $U(t)$, the same approximations as for the grid method can be used. They are usually faster when applied in the eigenstate basis, since the computational space can be limited to the relevant eigenstates.

2.2. Implementation of Quantum Logic

There exist two basic approaches to the implementation of quantum logic processes for quantum computations or simulations: *universal* quantum computing, which is based on a complete set of elementary quantum gates, and *precompiled* quantum computing, which relies on problem specific realizations of algorithms.

For *universal* quantum computing, laser fields must be optimized that result in elementary quantum gates through interaction with the system. The choice of elementary gate operations is arbitrary apart from the prerequisite that they constitute a complete set for the implementation of any desired unitary transformation. For example, in ion trap quantum computing, the universal set consists of single qubit flip and phase gates implemented by Rabi oscillations with highly phase stabilized continuous wave lasers and a controlled phase gate which is based on the utilization of an external degree of freedom (motional eigenstates of the ion array).[44] In NMR quantum computing, single qubit operations are also readily available by standard radio frequency pulse sequences. Also, a conditional phase gate, based on the *J*-coupling between nuclear spins, can be implemented, but on a different, longer time scale.[45] The proposal for molecular quantum computing developed in our group uses vibrational modes of polyatomic molecules to encode qubit systems[37] and belongs to the category of *universal* quantum computing. We were able to give the proof of principle to realize all elementary quantum gates necessary to perform logic operations and selected quantum algorithms,[38] and we have outlined strategies for experimental realization.[39,40] Single-qubit gates as well as two-qubit gates can be implemented within the same time scale by specially modulated ultrashort laser pulses.[39] For vibrational qubits, modulated femtosecond laser pulses in the infrared (IR) regime, which drive vibrational modes in the electronic ground state, are well suited.[36] An extension of this scheme to the UV/vis regime with vibrational eigenstates in electronically excited states is possible.[34] The femtosecond technique provides for significantly faster quantum gates than achieved in all other approaches.

The protocol of a computational process following the scheme of *universal* quantum computing consists of the following: (1) initialization of a qubit register in the state $|0000...0\rangle_n$; (2) implementation of a sequence of elementary quantum gates; (3) readout by a final, probabilistic measurement which collapses the system to one defined state. The readout from vibrational molecular qubits can be implemented by spectrally well resolved laser induced fluorescence measurement. The implementation of *universal* quantum information processing requires the precise switching of the population of the qubit states. Moreover, for elementary quantum gates to be applicable to any state that emerges during a quantum algorithm, phase control is essential. In the case of superposition states, the information is encoded in the relative phases between the basis states.

We speak of *precompiled* quantum computing, if quantum algorithms are not composed of elementary operations, but rather the complete algorithm (e.g., a quantum Fourier transform) is implemented in a problem specific way as one unitary transformation in one step. *Precompiled* quantum computing processes have been proposed mainly for molecular quantum computing with vibronic superpositions in electronically excited states, where the logic operations can be accomplished either by laser interaction or through the time dependent system dynamics.[31−33] Sometimes a special encoding of the input information is exploited to simplify gates and precedes the quantum gate or algorithm.[46] This relates to the fact that the implementation of the unitary transformation strongly depends on the representation of the logical qubit basis in the state space of the physical system and/or on the preparation step of an initial coherent superposition of qubit basis states. An advantage of exclusively using the coherences of rotational or vibrational eigenstates in a superposition to encode and process quantum information is that there is no need for exhaustive population transfer.[46] The result of such a quantum algorithm can be interrogated through wave packet interferometry or in general with a final short probe pulse (e.g., via pump−probe ionization transients[31]). The steps of initialization, computation, and readout can be merged into one process corresponding to well-known multipulse experiments, as has been proposed for DFWM (degenerate four-wave mixing) or TFRCARS (time−frequency resolved coherent anti-Stokes Raman scattering).[32,33]

Independent of whether the *universal* or *precompiled* ansatz is followed, coherent control is the basis of quantum information processing—either for the implementation of elementary quantum gates and of complete algorithms or for the preparation of special input states. In the next section,

we thus will outline the concepts of coherent control and optimal control theory.

3. Control of Molecular Quantum Systems

With the onset of laser technology in the 1960s, the idea of laser control of molecular vibrations was born. Initial suggestions focused on using intense narrow-band infrared radiation to selectively address vibrational modes in a specific chemical bond. However, this concept proved to be limited to only a few molecular systems, since the coupling between different degrees of freedom leads to very fast energy redistribution. Selective control can be induced in a molecular system by quantum interference. In this field of quantum control, the spectral−temporal properties of coherent light fields are adjusted to drive a given initial quantum state into a preselected target state. From a manifold of possible pathways, the optimal one is selected.

The first theoretical proposals for quantum control discussed three main control scenarios. The Brumer−Shapiro phase control scheme directly exploits interferences between different light-induced reaction pathways[47] by simultaneously applying two continuous wave (CW) laser fields of frequencies ω and 3ω. By this scheme, energetically degenerate final levels at an energy $3\hbar\omega$ can selectively be addressed. The second methodology is formulated in the time domain and was proposed by Tannor, Kosloff, and Rice.[48] It relies on the precise timing of wave packets prepared on an excited electronic state by a femtosecond laser pulse. The evolving wave packet screens several nuclear configurations and can be transferred back to the ground state when the desired product configuration has been reached. The third control scheme was suggested and realized by Bergmann and coworkers and is known as "stimulated Raman adiabatic passage" (STIRAP). It is a three-level control scheme and relies on a counterintuitive sequence of pump and probe pulses.[49] In these three concepts, a single parameter was varied, respectively, and different aspects of the common mechanism of light-controlled quantum interference are addressed. Optimal control theory (OCT) is designed to allow the simultaneous variation of multiple control parameters in a laser field, such as frequency, phase, and polarization, which are tunable also in an experiment.[50] Thus, it is the appropriate choice to study control mechanisms in complex quantum systems such as molecules. The theory of specifically shaped femtosecond laser pulses in the context of coherent reaction product control was already discussed by Tannor and Rice,[4] who used variational calculus to find the optimal fields. Rabitz and co-workers[5] and, independently, Kosloff and co-workers[6] have then established optimal control theory for many-parameter quantum control. In 1992, Judson and Rabitz[7] paved the way to experimental realization as they transferred the OCT concept to the experiment and suggested the new method of closed-loop control.

3.1. Optimal Control: Theory and Experiment

Optimal control theory (OCT) is a very powerful tool for calculating laser pulses, which will guide a quantum system to any selected objective. Possible objectives for molecular quantum systems are the preparation of specific eigenstates (electronic, vibrational, rotational), specifically shaped wave packets, or the localization of a wave packet in selected areas on a potential surface. As already mentioned, the control principle relies on the interaction of the electric field of the laser light with the quantum system via constructively and destructively interfering pathways. The electric field of a femtosecond laser provides the necessary flexibility of spectral and temporal properties to manipulate complex molecular processes. OCT has already been applied successfully to control ultrafast molecular reactions.[51−53]

The calculated pulses will not be perfect, due to necessary approximations in the system Hamiltonian and in the theoretical description of the environmental effects experienced in the experiment. Nevertheless, the main characteristics of the underlying control mechanism can be extracted and the question of controllability of the selected objective can be answered. Furthermore, the calculated laser field can be used as an intelligent initial guess for the control experiment.

The experimental analogue of OCT is the optimal control experiment (OCE) first suggested by Judson and Rabitz[7] and realized in a closed loop setup[54] that combines three main parts: a genetic algorithm for the generation of the various and increasingly optimized pulse forms, a pulse modulator (liquid crystal device (LCD), acousto-optic modulator (AOM), or flexible mirror) to realize the proposed pulse shapes, and the molecular probe itself. For LCD modulators, a mask function regulates the application of voltages to the individual LCD pixels. Thus, their diffraction index is spatially modulated, imprinting the pulse shape on a passing laser beam in the frequency domain. The mask function $M(\omega)$ is the direct interface between theory and experiment. It can be extracted from $\epsilon^{\mathrm{opt}}(\omega)$, the Fourier transformed frequency spectrum of the calculated optimized laser field, and a Gaussian spectrum $\epsilon^{\mathrm{FL}}(\omega)$ that encompasses the modulated spectrum $\epsilon^{\mathrm{opt}}(\omega)$ completely:[55]

$$M(\omega) = \frac{|\epsilon^{\mathrm{opt}}(\omega)|}{|\epsilon^{\mathrm{FL}}(\omega)|} \tag{4}$$

This theoretically evaluated function exposes the complexity of the control task and its realizability. It can be directly put on the pulse modulator and serves as an "intelligent" initial guess for an experimental closed loop setup.

3.2. Optimal Control Theory for Global Quantum Gates

The task of OCT in molecular quantum computing is highly demanding, since both multiple population transfer and the phase evolution have to be controlled. The optimal laser field $\epsilon(t)$ must drive a system from a set of initial states $\psi_{ik}(0) = \Phi_{ik}$ (index i) at a time $t = 0$ to multiple final target states Φ_{fk} (index f) at a fixed time $t = T$. The initial and target states correspond to the eigenstates defining the qubit basis. In case of vibrational qubits, the basis states can be either pure vibrational states or superposition states. The calculated laser pulse $\epsilon(t)$ represents the global quantum gate, and its fidelity is defined as[56]

$$\text{fidelity} = \frac{|\tau|^2}{N^2}$$

with

$$\tau = \sum_{k=1}^{N} \langle \Phi_{fk} | \psi_{ik}(T) \rangle \tag{5}$$

where N is the number of basis states and τ gives the overlap between the desired target states Φ_{fk} and the laser driven wave functions $\psi_{ik}(t)$ at the final time T. Algorithmic schemes allow the formulation of the optimization problem by maximization of the following multitarget optimal control (MTOCT) functional:

$$K(\psi_{ik}(t),\psi_{fk}(t),\epsilon(t)) = F(\tau) - \int_0^T \alpha(t)|\epsilon(t)|^2\,dt - \sum_{k=1}^{N} 2\mathrm{Re}\{C\int_0^T \langle\psi_{fk}(t)|(i/\hbar)[H_{sys} - \mu\epsilon(t) + (\partial/\partial t)]|\psi_{ik}(t)\,dt\rangle\} \quad (6)$$

The first term is the control aim with the target function $F(\tau)$, which is here set up as a function of τ. The target function $F(\tau)$ can be implemented in different ways, depending on the demands to be fulfilled by the control algorithm. The second term in eq 6 represents the laser field $\epsilon(t)$, which drives the system wave functions toward the target states. The field intensity is limited by the penalty function $\alpha(t) = \alpha_0/s(t)$. The overall shape function $s(t)$ satisfies the experimental demand of a smooth switch on and off behavior.[57] The penalty factor α_0 limits the time averaged laser intensity. The last term of eq 6 ensures that the time dependent Schrödinger equation is fulfilled at any point in time. H_{sys} is the time independent Hamiltonian of the molecule, and μ is the dipole moment vector field. The prefactor C depends on the choice of $F(\tau)$ and ensures the separability of the resulting set of differential equations after variation of the functional.

To find a maximum, the functional is varied with respect to its variables $\psi_{ik}(t)$, $\psi_{fk}(t)$ (Lagrange multipliers), and $\epsilon(t)$, and the search for $\delta K = 0$ leads to a set of $2N + 1$ coupled differential equations. This set of differential equations is solved iteratively using forward/backward propagation and results in one optimal laser field $\epsilon(t)$ as a self-consistent solution to this system.

Of highest importance for the application of OCT in the context of molecular quantum computing is the fact that the multitarget functional allows optimization of several transitions within the molecule simultaneously with the same laser pulse: A quantum gate has to operate correctly on each possible qubit state, and in general, this quantum state is unknown. To ensure this, the laser field has to drive the correct population transfer starting from each state of the standard qubit basis (in the following, this is referred to as "global population transfer"), and moreover, the phases between the standard basis states have to be set correctly. The key effect of the multitarget algorithm is to extract the characteristic features of single transitions and to combine them into one global pulse. Depending on the definition of $F(\tau)$, not only global population transfer is optimized but also the phase evolution can be controlled. In the following, we summarize three different formulations of $F(\tau)$ applied in the context of quantum computing.

Standard MTOCT. Global population transfer between qubit basis states can be obtained when the target function $F(\tau)$ is defined as

$$F(\tau) = \sum_{k=1}^{N} |\langle\psi_{ik}(T)|\Phi_{fk}\rangle|^2 \quad (7)$$

In this case, the prefactor C has the form

$$C = \langle\psi_{ik}(t)|\psi_{fk}(t)\rangle$$

This target definition allows the control of global population transfer but no phase control.

Phase Sensitive MTOCT. Global population and phase control for each target wave function can be achieved when the target function is defined as the real part of the overlap with the target state:

$$F(\tau) = \mathrm{Re}[\sum_{k=1}^{N} \langle\psi_{ik}(T)|\Phi_{fk}\rangle] \quad (8)$$

In this case, the prefactor C equals one. With a given equal global phase of all k target states Φ_{fk}, also the relative phases of the k laser driven states $\psi_{ik}(T)$ are correlated.

Phase Correlated MTOCT. A general OCT algorithm for the optimization of unitary transformations was derived by Palao and Kosloff.[56,58] Transferred to the MTOCT formalism of eq 6, the objective $F(\tau)$ now has the form

$$F(\tau) = |\tau|^2 = \sum_{k=1}^{N}\sum_{l=1}^{N} \langle\psi_{il}(T)|\Phi_{fl}\rangle\langle\Phi_{fk}|\psi_{ik}(T)\rangle \quad (9)$$

and C equals

$$C = \sum_{i=1}^{N} \langle\psi_{il}(t)|\psi_{fl}(t)\rangle$$

This formulation guarantees the relative phase correlation between all qubit transitions while the phase of the single transitions need not directly be addressed. The additional freedom introduced increases the flexibility of the algorithm and generally yields better results (for a detailed analysis, see ref 56). This method is closely related to a previous approach developed in our group, which uses additional superposition state transitions in the standard MTOCT.[38] In the following, we will present applications of the standard MTOCT and of the phase correlated variant for *universal* quantum computing.

4. Universal Quantum Computing with Vibrational Qubits

To analyze the requirements for pulse shaping techniques and for molecular properties, we select the approach of *universal* molecular quantum computing with vibrational qubits. A set of elementary quantum gates consisting of the single qubit operations NOT gate, Hadamard gate, and a phase gate (exemplarily a Π gate), plus a controlled-NOT (CNOT) gate as a two-qubit operation, has been chosen as examples. The essential elementary logic operations can be defined by the desired state-to-state transitions in the qubit basis. For example, in a minimal two-qubit basis, the optimized transitions for quantum gates acting on the second qubit are as follows:

$$\text{NOT: } |00\rangle \leftrightarrow |01\rangle \quad \text{and} \quad |10\rangle \leftrightarrow |11\rangle$$

$$\text{Hadamard: } |00\rangle \leftrightarrow \frac{1}{\sqrt{2}}(|00\rangle + |01\rangle),$$

$$|01\rangle \leftrightarrow \frac{1}{\sqrt{2}}(|00\rangle - |01\rangle), \quad |10\rangle \leftrightarrow \frac{1}{\sqrt{2}}(|10\rangle + |11\rangle),$$

$$\text{and} \quad |11\rangle \leftrightarrow \frac{1}{\sqrt{2}}(|10\rangle - |11\rangle)$$

$$\Pi\text{: } \frac{1}{\sqrt{2}}(|00\rangle + |01\rangle) \leftrightarrow \frac{1}{\sqrt{2}}(|00\rangle - |01\rangle) \quad \text{and}$$

$$\frac{1}{\sqrt{2}}(|10\rangle + |11\rangle) \leftrightarrow \frac{1}{\sqrt{2}}(|10\rangle - |11\rangle)$$

$$\text{CNOT: } |00\rangle \rightarrow |00\rangle, \quad |01\rangle \rightarrow |01\rangle, \quad \text{and} \quad |10\rangle \leftrightarrow |11\rangle \tag{10}$$

Depending on the size n of the qubit system, 2^n transitions (2×2^n for the Hadamard gate to ensure that it is self-inverse) have to be realized by one laser field, which induces the desired elementary quantum gate. Relative phase control, as is needed for the Hadamard and Π gates, is achieved by the introduction of superposition states in the optimized transitions as given in eq 10. If the phases of all transitions are correlated in the right way—as is the case, for example, for the Hadamard and the Π gate in eq 10—we call the corresponding gate or laser field *phase correct* or *phase optimized*. In case exclusively the right population transfer for all transitions is driven without special attention to the relative phases between them, we label the corresponding laser field or quantum gate simply *global*.

Employing different optimization targets (discussed in section 3.2) or state-to-state transitions, laser fields for either population control or population and relative phase control can be calculated. Since, in most system setups, population and phase development take place on different time scales, simultaneous control is the more challenging task. For the vibrational qubit setup, the population transfer between vibrational states can be accomplished within a few hundred femtoseconds to some picoseconds, while the development of the relative phases in superposition states is significantly faster by a minimum of 2 orders of magnitude (with a time scale of femtoseconds or even sub-femtoseconds). As a consequence, it is advantageous to first treat population and phase control separately. Detailed analyses have been carried out of how the two control goals can be achieved and how the implementation of essential quantum gates is influenced by different molecular properties and experimental constraints of the laser system.[36,37−40,59−64]

In the following, we will review the fundamental results of these investigations, with emphasis on the quantum gate laser pulse shapes and the corresponding mechanisms. Fault tolerant quantum computing requires extremely high accuracy, with errors below 10^{-4}.[65,66] The theoretical proof of principle to reach any desired fidelity with modulated femtosecond laser fields was given by Palao and Kosloff.[56,58] However, to reach this limit in calculations, computer time increases exponentially. In the corresponding coherent control experiment, the time to solve the Schrödinger equation is not a fundamental issue and depends only on the correct implementation of the feedback loop. For the following discussions of laser field shapes and mechanisms, this limit of accuracy is not pursued, as there are only negligible effects on general mechanistic features and trends observed, when the fidelity is driven above 99%.

4.1. Elementary Gate Operations: Population Control and Mechanisms

To obtain results which could easily be compared with spectroscopic data and transferred to an experiment, we have optimized and analyzed the set of elementary quantum gates in a systematic approach in parametrized, analytical model systems. We have identified the anharmonicity of the qubit normal modes and the coupling between the qubit normal modes as parameters with fundamental influence on the resulting pulse structure and have varied them individually in our optimization studies. The interplay of anharmonicity and coupling results in the rich structure of molecular vibrational eigenstates and in an increasing spectral density when turning to higher excitations.

Figure 3a shows population optimized laser fields for all elementary quantum gates of the selected universal set in a two-qubit model system. In this system, the second, active qubit normal mode has an anharmonicity of 43 cm^{-1} and the coupling between the two qubit normal modes is 8 cm^{-1}. In the following, model systems are labeled according to the scheme anharmonicity-coupling given in wavenumbers. Thus, the system considered here is referred to as system 43-8.

The elementary gates NOT, CNOT, Hadamard, and Π have been calculated for a minimum duration T needed to achieve a yield of >99%, as well as an experimentally feasible peak intensity in the range of 10^{10} W/cm^2,[62] which lies well below the ionization limit. Also displayed in Figure 3a are the mechanisms of population transfer, starting from the basis states $|00\rangle$ or $|10\rangle$ for NOT, CNOT, and Hadamard gates, and from $1/\sqrt{2}(|00\rangle + |01\rangle)$ and $1/\sqrt{2}(|10\rangle + |11\rangle)$ for the Π gate. The time integrated frequency spectra of the specially shaped laser pulses are depicted in Figure 3b, together with the excitation frequencies for desired qubit transitions in black and the spectral region of undesired overtone transitions in gray.

All elementary quantum gate laser fields show a multipulse substructure. The longest and most complex laser field arises for the Hadamard gate with the most demanding optimization task of population and relative phase control. For NOT, CNOT, and Π gates, the short subpulses interfere in the frequency domain such that qubit transition energies and overtone excitations are spectrally well resolved (see drops in intensity in the frequency spectra, Figure 3b). Thus, NOT, CNOT, and Π gates work without significant overtone excitation, in contrast to the Hadamard gate. Their mechanisms are correspondingly simple. On the other hand, all spectra in Figure 3b, especially those of the NOT, CNOT, and Π gates, show an overhead of superfluous frequencies. This results from the fact that the shortest possible quantum gate implementations were optimized, which yields sequences of relatively short and thus broad-band subpulses. The superfluous frequencies are blue-shifted, beyond the range of any possible transitions, to avoid undesired laser−molecule interaction. To provide a physical interpretation of the quantum gate laser field structures, we will elucidate the mechanistic aspects in more detail.

NOT. For a NOT gate, the active qubit has to be flipped irrespective of the values of all other qubits. Accordingly, in an n-qubit system, 2^n transitions with 2^{n-1} slightly different excitation energies have to be driven while overtone transitions have to be avoided. The spreading of the qubit transition frequencies for different values of the passive qubit(s) and their separation from the overtone excitation energies depend

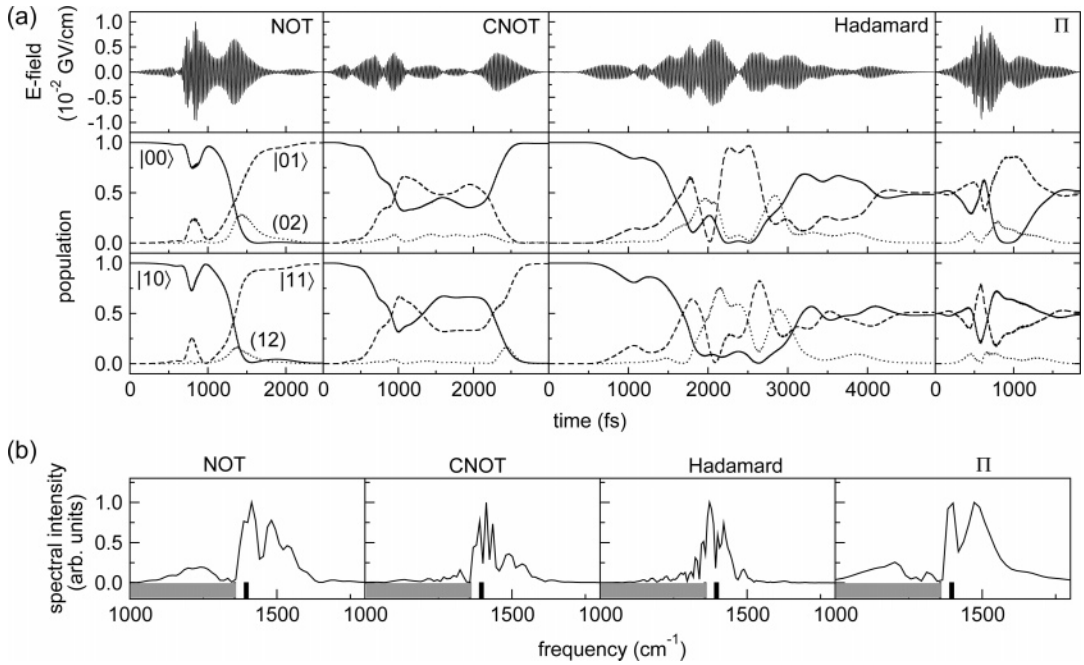

Figure 3. Universal set of elementary quantum gates in the model system 43-8: (a) laser fields (top row) with two selected mechanisms below; (b) spectral intensity of the quantum gate laser fields. The overtone region is marked in gray, and the qubit transitions are indicated as black bars.

on the molecular parameters coupling and anharmonicity. The presented NOT laser field in the system 43-8 is almost time symmetric. The first prominent subpulse in combination with two intense but very short subpulses merely effects a slight population oscillation. Here, the transition frequencies $|00\rangle \leftrightarrow |01\rangle$ and $|10\rangle \leftrightarrow |11\rangle$ are similar enough for the switching process to be carried out in one step during the second prominent subpulse. More complex mechanisms might occur in higher dimensional systems (see section 4.3) or systems with different relative magnitudes of anharmonicity and coupling (see section 4.2).

CNOT. For a controlled two-qubit flip gate, the specially shaped laser field also needs to distinguish between the transitions within the qubit basis, in a way that the active qubit is only flipped when the passive qubit is in the defined state. The selective addressability of the corresponding transitions is enabled through their slightly shifted excitation energies due to the coupling between normal modes. We interpret this interaction between qubit normal modes as "inherent entanglement", which allows for a straightforward implementation of two qubit gates like the CNOT gate.[62] Thus, in a molecular vibrational qubit setup, multiqubit gates like the CNOT or the Toffoli gate are in general realized more easily with a single laser molecule interaction than in a setup which uses external degrees of freedom (i.e., vibrational modes addressed in an ion trap setup to activate the interaction between single ions). For example, the CNOT gate laser field in the two-qubit system 43-8 selectively drives the transition $|10\rangle \leftrightarrow |11\rangle$, while the states $|00\rangle$ and $|01\rangle$ are not switched (see Figure 3a, second panels). The two transition frequencies $|00\rangle \leftrightarrow |01\rangle$ and $|10\rangle \leftrightarrow |11\rangle$ are spectroscopically not resolved in the laser field spectrum (see Figure 3b), and intermediate population transfer results also for the initial states $|00\rangle$ and $|01\rangle$. Still, the correct switching process is accomplished at the end of the laser pulse sequence due to the different relative phase development in the intermediate superposition states $1/\sqrt{2}(|00\rangle + e^{i\phi_1}|01\rangle)$ and $1/\sqrt{2}(|10\rangle + e^{i\phi_2}|11\rangle)$ and a correspondingly different action of the laser pulse sequence.

Hadamard. As already stated, the Hadamard gate in the two-qubit model system displays the most complex mechanism. At first sight, the Hadamard gate should be the simplest elementary gate, since the switching processes of a NOT gate have to be implemented only halfway.[60] However, taking into account the right relative phase development and also ensuring that the Hadamard gate is self-inverse result in a much more complicated optimization task. For the minimum duration of the Hadamard gate operation in the system 43-8, no spectral discrimination of the desired qubit transitions from the undesired transitions to the first overtones (02) and (12) is achieved. As a consequence, the mechanism involves strong population oscillations and also extensive overtone excitation. This comparatively rich structure is necessary to achieve the desired population and relative phase control.

Π Gate. Phase gates like the Π gate demand for the control of the phases of individual qubit basis states (i.e., their relative phases in a superposition state) without need for population transfer. Nevertheless, they can be implemented by laser interaction. The corresponding mechanism relies on population transfer and interference of different pathways starting from the various qubit basis states. When the phase gate laser fields are applied on superposition states, only intermediate population transfer occurs, as depicted in Figure 3a for the Π gate in the system 43-8. Accordingly, most Π gates optimized for superposition state to superposition state transitions result in net population transfer if they are applied on pure basis states. Since such phase gates only work correctly with superposition states, technically they are not basis set independent. A practical alternative to laser-induced phase shifts is to use simply the free phase evolution of basis states (in superpositions), as will be discussed in section 4.4.

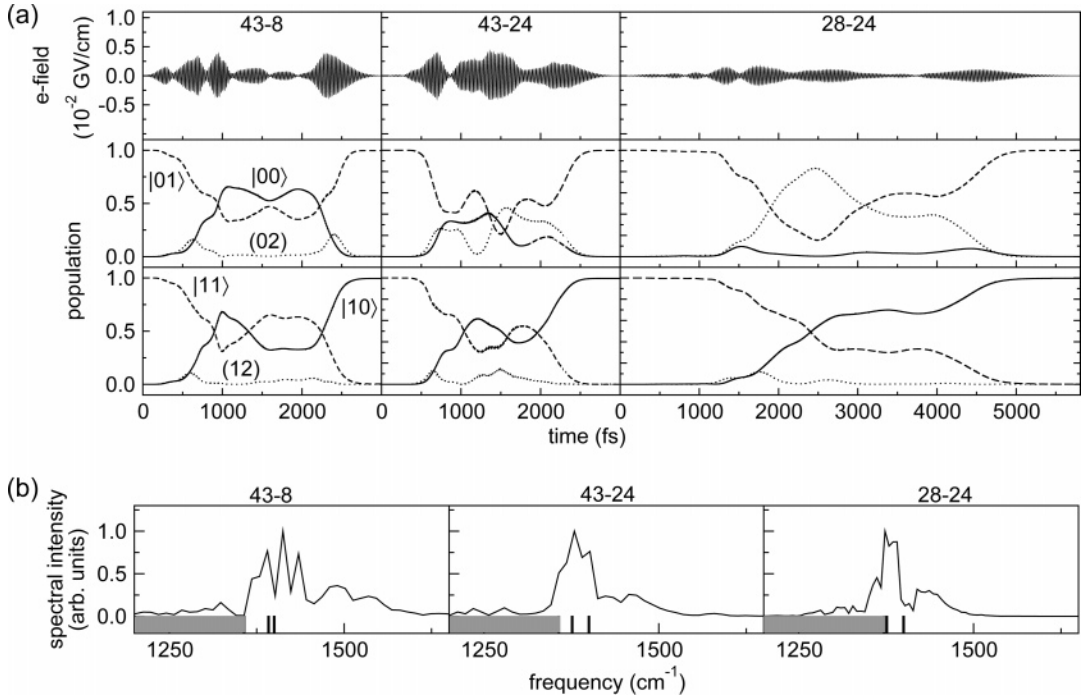

Figure 4. CNOT laser fields for different model systems with varying anharmonicity and coupling: (a) laser fields (top row) with two selected mechanisms below; (b) spectral intensity of the quantum gate laser fields. The overtone region is marked in gray, and the qubit transitions are indicated as black bars.

4.2. Influence of Molecular Parameters

The quantum gate laser field structures discussed above are based on one specific model. Nevertheless, some general features can be retrieved for all systems tested. From our systematic investigations in various model systems with different molecular parameters, it has become evident that the complexity of a quantum gate implementation depends sensitively on the interplay of anharmonicity and coupling,[62] parameters that have been introduced in section 4.1. The anharmonicity defines the spectral separation from the overtone ladders of the individual qubit modes[60,62] and provides for a more or less isolated two-level system. Consequently, a high anharmonicity is desirable and facilitates the implementation of all elementary quantum gates. The selective addressability of the transitions within the qubit basis is determined by the coupling between the qubit normal modes. The net effect of the coupling on the quantum gate complexity depends on its magnitude relative to the anharmonicity; that is, a big ratio of anharmonicity/coupling generally yields simpler quantum gate laser fields and mechanisms.[62] This is easily understood for NOT, Hadamard, and phase gates, for which the spectral separation from overtone transitions plays the decisive role. For such one-qubit gates, close lying qubit transition frequencies are favorable. An extension of this scheme to the CNOT gate, which depends on the switching condition given by the coupling, is not immediately evident. However, the trend of a favorably high ratio of anharmonicity to coupling can be understood from the analysis of the quantum gate complexities and mechanisms in model systems with different parameters.

Figure 4 displays examples of laser fields with minimum durations and a yield of >99% for the CNOT gate in different two-qubit model systems, together with their mechanisms starting from $|01\rangle$ and $|11\rangle$ in part 4a. In Figure 4b, the frequency spectra of the laser fields are presented, with the qubit transition frequencies marked in black and the range of overtone transition frequencies marked in gray. The CNOT laser field for the model system with high anharmonicity and small coupling (43-8) and the corresponding mechanisms have already been discussed in the previous section. Because of the small coupling, the $|00\rangle \leftrightarrow |01\rangle$ transitions cannot be spectrally resolved from the desired $|10\rangle \leftrightarrow |11\rangle$ transitions, and a selective switching process is enabled by the phase evolution of the superposition states generated intermediately. A substantially higher coupling, which allows for spectral resolution of the desired and undesired qubit transitions, does not necessarily result in a less complex laser field structure or simpler mechanisms. This is shown exemplarily with the system 43-24 in Figure 4. Here, the frequency for the desired $|10\rangle \rightarrow |11\rangle$ transition lies equally well separated from that of the undesired $|00\rangle \leftrightarrow |01\rangle$ qubit transition and that of the (02) overtone excitation starting from $|01\rangle$. As a consequence, the shortest possible laser field contains all three frequencies and a more complex mechanism with intermediate overtone excitation results. For the case of similar magnitudes of anharmonicity and coupling, as in the third system 28-24 in Figure 4, a discrimination between $|00\rangle \leftrightarrow |01\rangle$ and $|10\rangle \leftrightarrow |11\rangle$ transitions by spectral resolution is obtained, while the frequency for the $|10\rangle \leftrightarrow |11\rangle$ transition and the overtone excitation $(01) \leftrightarrow (02)$ almost coincide. A selective switching process is again accomplished by virtue of the different relative phase evolutions of intermediate superposition states $1/\sqrt{2}(|01\rangle + e^{i\phi_1}|02\rangle)$ and $1/\sqrt{2}(|10\rangle + e^{i\phi_2}|11\rangle)$. The duration of the corresponding CNOT laser field is significantly increased compared to the systems with higher anharmonicity/coupling ratio.

As a general aspect, different transitions can be distinguished not only spectroscopically but also via the slightly different relative phase evolution of intermediate superposition states.[62] Thus, where no spectral resolution for a given laser field duration is possible, a discrimination of desired

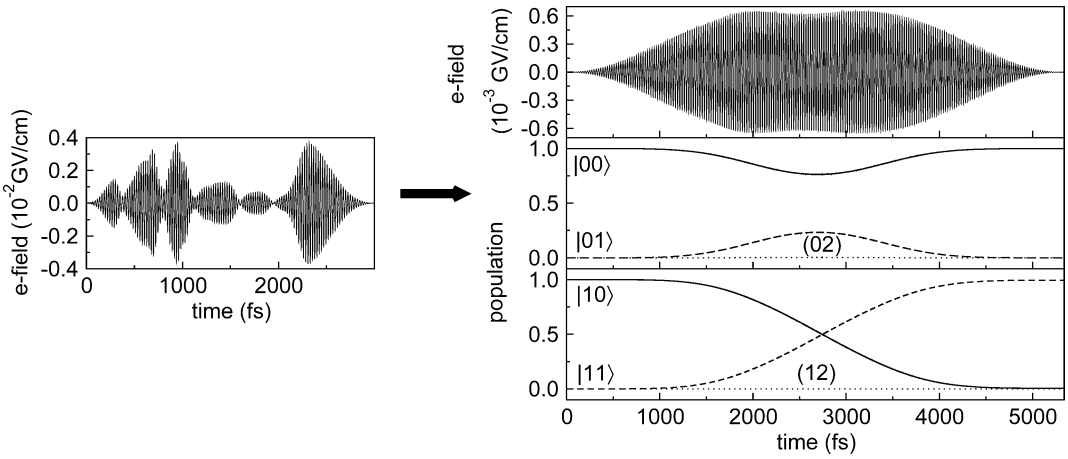

Figure 5. CNOT laser fields optimized for two different durations *T*: (left side) minimum duration; (right side) "optimal" duration, with two selected mechanisms.

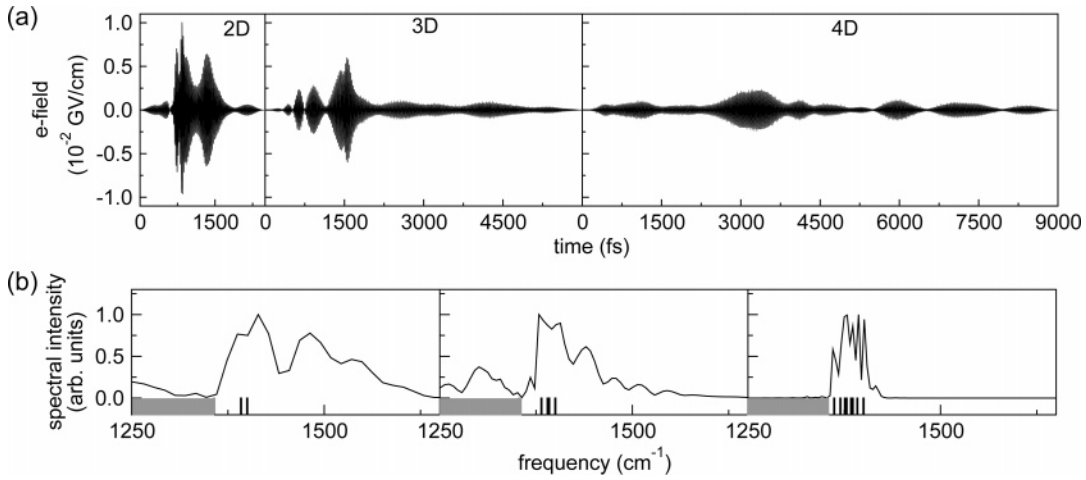

Figure 6. NOT gate laser fields for higher dimensional systems: (a) laser fields for 2D, 3D, and 4D systems; (b) the corresponding spectra with overtone regions marked in gray and the qubit transitions indicated as black lines.

and undesired qubit or overtone transitions is achieved by interference of different pathways, that is, the effect of different interaction of intermediate superposition states with the same pulse sequence.

So far, quantum gate laser fields with the shortest possible durations necessary for appreciable fidelities >99% have been presented. They all consist of a sequence of shorter, partially overlapping subpulses with a correspondingly broad frequency distribution. As expected, with longer gate durations *T*, which allow also for longer subpulses and a better frequency resolution, extremely simply shaped quantum gate laser fields and one-step adiabatic mechanism can be obtained.[62] Exemplarily, this is shown for the CNOT gate in the model system 43-8 in Figure 5. The laser field with a duration of 5500 fs displays an extremely simple structure of two strongly overlapping subpulses. This is a very prominent pulse sequence for CNOT gates, which was found for various molecular systems with different parameters.[39,40,62] Such a pulse structure should be realizable straightforwardly with state-of-the-art experimental techniques (see section 6). More complex structures will be attainable in the IR regime as soon as direct shaping with masks in the frequency domain has become a standard laboratory technique in this spectral region. In conclusion, there is a choice between short, strongly modulated quantum gate laser fields and longer, simply structured pulse trains.

4.3. Quantum Gates in Higher Dimensional Systems

The influence of molecular parameters also enters the scaling of the quantum gate complexity with the dimension of the qubit system. We have investigated this dependency of the quantum gate complexity in some three- and four-qubit model systems, for which we calculated the essential quantum gates NOT, CNOT, and Hadamard with the shortest possible durations. From this set, we constructed a sequence to prepare a maximally entangled three-qubit GHZ state.[64]

Figure 6 shows for comparison NOT gate laser fields on the last qubit with minimum duration, for yields of >99% in the cases of the two- and three-qubit systems and <92% in the case of the four-qubit system. The optimized transitions are

$$\begin{aligned} |000\rangle &\leftrightarrow |001\rangle \\ |010\rangle &\leftrightarrow |011\rangle \\ |100\rangle &\leftrightarrow |101\rangle \\ |110\rangle &\leftrightarrow |111\rangle \end{aligned} \tag{11}$$

in the three-qubit system, and

$$
\begin{aligned}
|0000\rangle &\leftrightarrow |0001\rangle \\
|0010\rangle &\leftrightarrow |0011\rangle \\
|0100\rangle &\leftrightarrow |0101\rangle \\
|1000\rangle &\leftrightarrow |1001\rangle \\
|0110\rangle &\leftrightarrow |0111\rangle \\
|1010\rangle &\leftrightarrow |1011\rangle \\
|1110\rangle &\leftrightarrow |1111\rangle
\end{aligned} \tag{12}
$$

in the four-qubit system.

For an increasing number of qubits, in compliance with an increasing pulse duration and a more defined pulse structure, the superfluous red- and especially blue-shifted spectral intensity parts diminish. This can again be explained by the influence of anharmonicity and coupling. For a flip gate on one qubit, like NOT and Hadamard, the 2^{n-1} slightly different transition frequencies ω_k, which have to be driven simultaneously, require an increasing spectral bandwidth of the driving laser pulse as the size of the qubit system increases. Due to the coupling between normal modes, however, the spectral separation between the qubit transitions (Figure 6a, in black) and overtone transitions (Figure 6b, in gray) decreases and the frequency modulation needs to be very sharp in this region. Correspondingly, longer pulse sequences result from the optimization to ensure selective addressability of the qubit transitions.

For the CNOT gate or any other controlled gate, the respective qubit transitions would have to be resolved in addition. In a three-qubit system, for example, the CNOT gate acting on the third qubit, and with the second qubit as control qubit, needs to distinguish between the desired $|010\rangle \leftrightarrow |011\rangle$ and $|110\rangle \leftrightarrow |111\rangle$ transitions and the undesired $|000\rangle \leftrightarrow |001\rangle$ and $|100\rangle \leftrightarrow |101\rangle$ transitions. The CNOT implementation then sensitively depends on the difference of the coupling parameters between qubits two and three and qubits one and three, since this determines the separation of the $|010\rangle \leftrightarrow |011\rangle$ and $|100\rangle \leftrightarrow |101\rangle$ transition frequencies. For a controlled three-qubit operation, that is, the Toffoli gate, the situation in a three-qubit system is less demanding, since, in correspondence to a CNOT gate in a two-qubit system, only the $|110\rangle \leftrightarrow |111\rangle$ transition needs to be selectively driven.[64]

In conclusion, turning to higher dimensional systems, the same parameters are important and the same rules apply that have been extracted for the two-qubit systems. Moreover, the feasibility of quantum gates in multiqubit systems depends strongly on the ratio of anharmonicity of the active qubit mode compared to the sum of coupling parameters which enter the excitation energy of the maximally excited qubit state $|1...1\rangle$. The control task of two-qubit gates becomes increasingly complex in more than two-dimensional qubit systems, as the spectral positions of desired and undesired transitions alternate. Correspondingly, the most effective CNOT mechanism here does not rely on spectral resolution, but once more on the different phase evolutions of intermediate superposition states.[64]

4.4. Phase Control and Phase Evolution

The phase development of qubits encoded in vibrational levels of molecules differs from that in implementations using identical physical systems for the respective qubits such as atoms in cavities and ions in traps. The inherent entanglement, which is due to the coupling between normal modes, on the one hand, enables the straightforward implementation of two-qubit (entangling) gates. On the other hand, the slightly different transition energies within the qubit basis result in a rather complex relative phase evolution in superposition states. The role of phase development and phases has been discussed extensively in refs 38 and 63. In the following, we will briefly explain the specific aspects of the phase evolution of vibrational molecular qubits and how to control it or utilize it for the implementation of phase gates. For comparison and completeness, we also elucidate the importance of relative phases and their evolution for the concept of *precompiled* quantum computing with rovibrational and electronically excited states.[31,33,46]

The free phase evolution of each state of a vibrational n-qubit basis is governed by its distinct eigenenergy:

$$\hat{U}(t-t_0)|(1...n)_k\rangle = \mathrm{e}^{i\omega_k(t-t_0)}|(1...n)_k\rangle \tag{13}$$

Consequently, the relative phase evolution of a superposition state $\Psi(t_0) = \sum_{k=1}^{2^n} c_k|(1...\ n)_k\rangle$ of n qubits is governed by the eigenenergies, or rather by the eigenenergy differences of the k involved standard basis states. This rapid relative phase development can be visualized by the autocorrelation function of a superposition state:[63]

$$|\langle\Psi(t_0)|\hat{U}(t-t_0)|\Psi(t_0)\rangle|^2 = \sum_{k=1}^{2^n}|c_k|^4 + \sum_{k=1}^{2^n}\sum_{l>k}^{2^n} 2|c_k|^2|c_l|^2 \cos(\Delta\omega_{kl}(t-t_0)) \tag{14}$$

The free evolution of the relative phases in superposition states during a defined time interval $\Delta t = t - t_0$ can also be interpreted as a specific phase gate $\hat{U}_{\phi k}$ and used as part of a quantum algorithm. The fidelity of a desired phase gate is then easily derived from[63]

$$|\langle\Psi(t_0)|\hat{U}_{\phi_k}{}^{\dagger}\hat{U}(\Delta t)|\Psi(t_0)\rangle|^2 = \sum_{k=1}^{2^n}|c_k|^4 + \sum_{k=1}^{2^n}\sum_{l>k}^{2^n} 2|c_k|^2|c_l|^2 \cos(\Delta\omega_{kl}\Delta t + \Delta\phi_{kl} - \Delta\theta_{kl}) \tag{15}$$

with the relative phases $\Delta\theta_{kl}$ of the initial states and $\Delta\phi_{kl}$ of the target states. The maxima of the functional in eq 15 give an optimal duration Δt for the desired phase gate. Such free evolution phase gates can be used either to implement pure, conditional phase gates, such as the Π gate or the phase gate needed for a quantum Fourier transform (see section 5), or to ensure the phase correctness of globally optimized laser fields, as we will demonstrate in the following.

During the impact of a laser field, which induces a specific quantum operation, say a CNOT gate, the phase evolution of qubit states depends on the phase of the laser pulse. In general, the relative phase evolution during a CNOT gate in a two-qubit basis is for each qubit state as follows:

$$
\begin{aligned}
|00\rangle &\rightarrow \mathrm{e}^{-i\phi_{00}}|00\rangle \\
|01\rangle &\rightarrow \mathrm{e}^{-i\phi_{01}}|01\rangle \\
|10\rangle &\rightarrow \mathrm{e}^{-i\phi_{11,\mathrm{laser}}}|11\rangle \\
|11\rangle &\rightarrow \mathrm{e}^{-i\phi_{10,\mathrm{laser}}}|10\rangle
\end{aligned} \tag{16}
$$

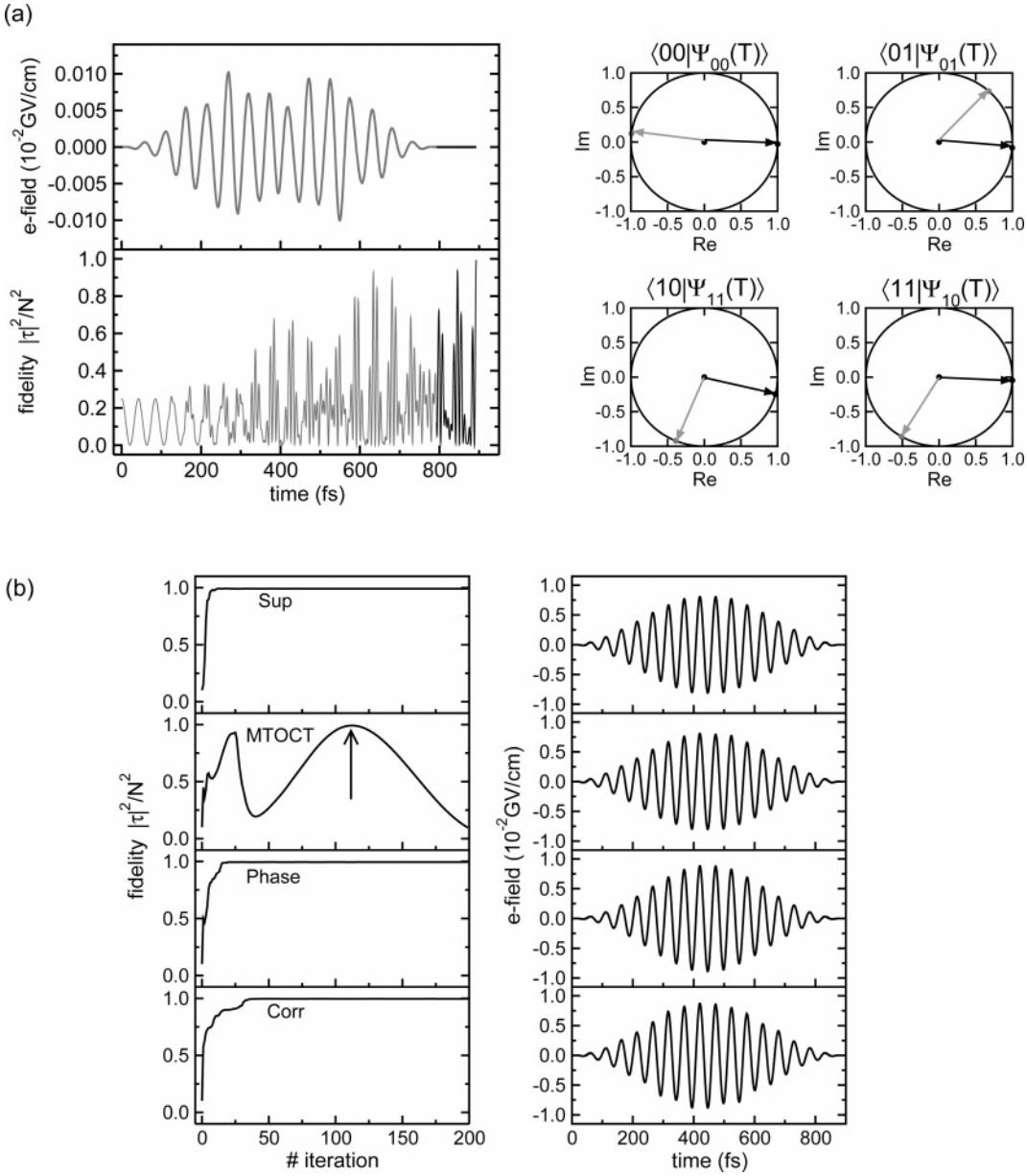

Figure 7. Phase correct CNOT gate in the 2D acetylene model: (a) The left, top panel shows the construction from a laser field optimized for global population transfer (gray) and a defined delay (black). The graph below displays the evolution of the gate fidelity according to eq 5. To the right, the projections of the laser-driven initial states onto the target states are represented in the complex plane after the laser field (gray) and after the delay (black). (b) Direct optimization of phase correct CNOT laser fields with different optimization targets and the optimal duration T from Figure 6a. The left panels show the development of the quantum gate fidelity, and the right panels show the laser fields of the final iteration, except for the case of MTOCT (second from top). Here the laser field with highest fidelity at iteration number 112 (indicated by the arrow in the left panels) is selected.

Starting from a maximum superposition state in a two-qubit basis, $^1/_2(|00\rangle + |01\rangle + |10\rangle + |11\rangle)$, this results in a superposition state with the corresponding relative phases:

$$\frac{1}{2}(|00\rangle + |01\rangle + |10\rangle + |11\rangle) \rightarrow e^{-i\phi_{00}}|00\rangle + e^{-i\phi_{01}}|01\rangle + e^{-i\phi_{11,\mathrm{laser}}}|11\rangle + e^{-i\phi_{10,\mathrm{laser}}}|10\rangle \quad (17)$$

The phases ϕ_{00} and ϕ_{01} are determined by the free evolution of the respective eigenstates, while the laser-driven states $|10\rangle$ and $|11\rangle$ exhibit phases $\phi_{11,\mathrm{laser}}$ and $\phi_{10,\mathrm{laser}}$ which additionally depend on the laser pulse phase and the driven states. Corresponding considerations apply to NOT, Hadamard, and Π gates.

For the successful application of elementary quantum gates in any sequence or quantum algorithm, the individual quantum gates need to be phase correct. This means that, up to an arbitrary global phase ϕ_g, the phases of all transitions need to be exactly controlled, as given by the unitary matrix of a quantum gate. For our example, of the two-qubit CNOT gate, the phases in eq 17 must meet the condition $\phi_{00} = \phi_{01} = \phi_{11,\mathrm{laser}} = \phi_{10,\mathrm{laser}} = \phi_g$. This is not guaranteed for *global* quantum gates, as is exemplified for the CNOT laser field displayed in gray in Figure 7a. It has been optimized with the MTOCT functional and for the transitions of eq 10 and induces the right population transfer with a yield of >99% (reflected in the unit length of the gray arrows in Figure 7a). However, the phase development, shown in Figure 7a by means of the complex coefficients of the overlap between target wave functions Φ_k and laser driven wave functions $\Psi_k(T)$, is different for each of the four transitions (gray

arrows). All arrows point into a different direction; that is, the phase development is different for each of the four transitions ($\phi_{00} \neq \phi_{01} \neq \phi_{11,\text{laser}} \neq \phi_{10,\text{laser}}$), and due to this, the fidelity (eq 5) of the corresponding CNOT gate is only ~12%. One can, however, compensate for this arbitrary phase development by an additional, well-defined delay, during which the relative phases freely develop according to eq 13 and are finally synchronized as desired. In the case of the CNOT gate considered in Figure 7a, after a delay of 100 fs following the laser field interaction, all phases in the qubit basis are adjusted in the right way, $\phi'_{00} = \phi'_{01} = \phi'_{11,\text{laser}} = \phi'_{10,\text{laser}}$, and collapse to one global phase ϕ_g. The sequence of laser field and free evolution results in an altogether phase correct CNOT implementation and a rise in fidelity to >99%. This is shown in Figure 7a, in black, respectively.

In section 3.2, we have introduced different functionals to optimize phase correct elementary quantum gates. In practice, it is not a simple task to optimize population and phase control simultaneously. Even relative phase control is a harder task than pure population control, as can be deduced from a comparison of Hadamard and NOT gates for a specific system (see section 4.1)—the Hadamard laser fields are much more complex or have an increased duration. This is based on the fact that the relative phase development takes place within femtoseconds, on the order of the time scale of the driving laser field oscillations. Thus, the total duration T in eq 6 is an extremely sensitive optimization parameter. As a consequence, for most "preselected" T, more complex laser fields result for *phase optimized* quantum gates than for *global* quantum gates and each optimization algorithm (eq 6 to eq 9) converges to different results. However, there exists an optimal duration T, for which the same simply structured laser field and a high fidelity for the corresponding quantum gate are received from all algorithms. This optimal time T can be deduced from the duration for a *global* laser field plus the subsequent time delay needed for the right phase synchronization during free evolution. Figure 7b shows time optimized runs for the CNOT gate in the system used in Figure 7a, with three different types of optimization algorithms (the multitarget state-to-state algorithm is used twice, with superpositions as "Sup" and without as "MTOCT"). For this optimal time, all algorithms yield the same phase optimized laser field with a fidelity of >99%. Even with the phase insensitive MTOCT algorithm, intermediately the phase correct laser field is found (iteration 112). This is indicated by the arrow in Figure 7b, left panel; the corresponding laser field is shown in Figure 7b, right panel. The following iterations only change the phase of the laser field, and thereby, the fidelity starts to oscillate. This already hints at the fact that the correct action of a quantum gate laser field in a sequence delicately depends on the stabilization of its phase.

The principle of "coherent control" relies on the interplay of the phases of molecular quantum states and that of the laser field. If in a sequence of quantum gates the phase of one laser pulse is shifted with respect to the others, its action on the intermediate qubit superposition state is altered. As a consequence, the result is tampered with. The effect of a shifted phase of one pulse can be counterbalanced by additional delays, such that the phase relations of the qubit basis states in superpositions are matched to the phase of the next laser pulse, and the desired operation is retrieved.[63] The implementation of quantum algorithms by sequences of shaped pulses for global population transfer plus intermediate delays for phase synchronization provides a very flexible tool kit. Still, for a quantum algorithm to work reliably, a highly sensitive phase stabilization of individual quantum gate laser fields is necessary. The techniques for phase stabilization of short laser pulses have recently been developed.[67,68] Due to the rapid and complex relative phase development within the qubit basis, also the synchronization of consecutive laser pulses needs to be very precise. The time scale lies in the regime of sub-femtoseconds to a few femtoseconds, since all relative phases of basis states in a superposition have to be exactly set. This task of phase control becomes increasingly complex in higher dimensional qubit systems. For a simplified and more robust approach, only the phases between those basis states coupled by the next quantum gate laser pulse need to be synchronized.[63] This corresponds to a projection of the phase space onto that of the single relevant qubit, which is addressed in the next quantum gate. Moreover, it denotes a transition to *precompiled* quantum computing, as such a sequence cannot be divided into overall phase correct elementary gates any more.

For *precompiled* quantum computing, the relative phase and its evolution in a superposition of molecular states, that is, a molecular wave packet, also plays the decisive role. In the approaches presented by Bihary et al.,[33] Vala et al.,[31] and Teranishi et al.,[46] a phase modulated laser pulse is applied to form a wave packet with information encoded in the defined relative phases. Either the laser field serves as the quantum algorithm itself,[31,33] or the initial wave packet is prepared in a special way, such that the quantum algorithm can be implemented solely by the free evolution of the system.[46] In the latter case, a different encoding of the qubit logical states in rovibrational superpositions is necessary and is given by the transformation matrix u_{CNOT} that diagonalizes the desired unitary transformation, for example, for a CNOT gate in a two-qubit basis:

$$\text{CNOT}_{\text{diag}} = u_{\text{CNOT}}{}^{-1}\begin{pmatrix}1&0&0&0\\0&1&0&0\\0&0&0&1\\0&0&1&0\end{pmatrix}u_{\text{CNOT}} = \begin{pmatrix}1&0&0&0\\0&-1&0&0\\0&0&1&0\\0&0&0&1\end{pmatrix} \quad (18)$$

In conclusion, molecular vibrational quantum computing can be viewed as a wave packet interferometry experiment. For *universal* quantum computing, the relative phases between laser pulses in a sequence of elementary quantum gates are important, and thus, the laser fields must be phase stable and well synchronized in time (including the delays). For the examples of *precompiled* quantum computing given so far, the global or absolute phase of the laser pulses, which prepare the input information, is not important but only the relative phases of spectral components, which are imprinted in the prepared wave packet. This, of course, is an advantage for *precompiled* quantum computing. However, it is unclear how increasingly complex quantum algorithms can be realized within the *precompiled* approach.[46]

5. Examples of Quantum Algorithms

The implementation of some touchstone algorithms already has been demonstrated or even realized experimentally using femtosecond laser techniques as quantum gates on qubits encoded in internal motional states of molecules.[31,33,38,63] Referring to the example of vibrational quantum computing with polyatomic molecules, Figure 8 shows theoretical

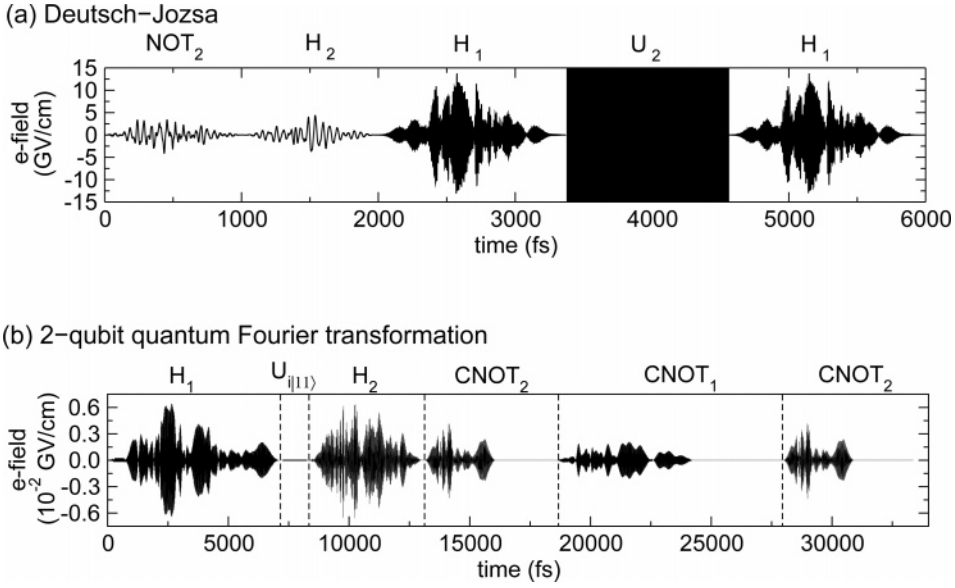

Figure 8. Pulse sequences for quantum algorithms on vibrational qubits: (a) Deutsch−Jozsa sequence; (b) the quantum Fourier transformation.

realizations of a two-qubit Deutsch−Jozsa (DJ) algorithm (Figure 8a)[38] and a two-qubit quantum Fourier transform (QFT) (Figure 8b)[63] in different qubit systems.

The DJ algorithm allows us to extract an essential feature of an unknown function of one (n) bit(s) by measuring only once ($2n + 1$ times), while any classical algorithm would require at least two ($2^{n-1} + 1$) measurements. The action of the unknown functions is encoded in an oracle transformation $\mathbf{U}_2$. The DJ sequence in Figure 8a has been calculated for the model system acetylene introduced in section 2.1.1. In this sequence, *phase optimized* laser fields have been used to implement the quantum gates. The index denotes the qubit each gate acts on. The oracle function $\mathbf{U}_2$ is represented by a NOT or Identity gate for constant functions and by a CNOT or ACNOT gate (with reversed switching conditions) for balanced functions. The probability for measuring the right outcome in the presented sequence is >94%. Errors stem from the accumulation of small deviations from the ideal implementation (100% fidelity) of the individual elementary quantum gates, which have been optimized with fidelities between 95% and 99%. An alternative scheme using electronically excited vibrational states has been proposed by Ohtsuki.[34]

The QFT is an essential ingredient in quantum algorithms, which rely on the extraction of the periodicity of a function or the so-called phase retrieval, with one prominent example being Shor's factoring algorithm. The QFT sequence in Figure 8b has been optimized exemplarily for the two-qubit model system 43-8. The Hadamard gates have been optimized phase correctly, while the CNOT gates are implemented with population optimized laser fields plus a defined delay to synchronize all phases. The conditional phase gate $\mathbf{U}_{i|11\rangle}$

$$\mathbf{U}_{i|11\rangle} = \begin{pmatrix} 1 & 0 & 0 & 0 \\ 0 & 1 & 0 & 0 \\ 0 & 0 & 1 & 0 \\ 0 & 0 & 0 & e^{i\pi/2} \end{pmatrix} \tag{19}$$

is implemented solely via the relative phase development during the free evolution between the two Hadamard gates. The fidelity of the total sequence is >99%, corresponding to the high fidelity of the individual quantum gates of >99%. This emphasizes the fact that, disregarding any external error sources, a high fidelity of quantum algorithms can be guaranteed by a precise optimization of the individual quantum gates.

6. Experimental Realization Strategies

In section 3.1, we have already addressed the generation of highly modulated laser pulses with very complex structures in various coherent control experiments. The majority of these experiments has used laser pulses in the UV/vis region, which can be formed with state-of-the-art, direct shaping techniques. Amplitude and phase masks are applied to LCDs, AOMs, and deformable mirrors for modulation in the frequency domain. Thus, *precompiled* quantum computing with rovibrational states in electronically excited molecules should be straightforwardly realizable experimentally.[45] The implementation of a DJ algorithm in a corresponding scheme has already been demonstrated by Vala et al.[31]

In the IR regime, direct shaping in the frequency domain has not been possible for a long time, and as yet, only simply shaped structures are available. Pulse trains with defined relative phases and delays are now accessible through direct and indirect shaping methods explained in refs 69−71.

For *universal* quantum computing with vibrational qubits, we found that all quantum gate laser fields are constituted by a sequence of partially overlapping subpulses (see section 4.1). With appropriate optimization parameters, simply structured pulse trains $\epsilon(t)$ can be obtained, which should be realizable straightforwardly in an experiment (see section 4.3):

$$\epsilon(t) = \sum_k \epsilon_{0,k} e^{-((t-t_{0,k})/\tau_{G,k})^2} \cos(\omega_{0,k}(t - t_{0,k}) + \varphi_{\mathrm{CEP},k}) \tag{20}$$

The decisive parameter for the correct action of a pulse train is the relative phase relation between the individual subpulses.[39] It consists of the subpulse carrier-envelope phases $\varphi_{\mathrm{CEP},k}$ plus the phases additionally introduced during their delays by $\omega_{0,k}(t-t_{0,k})$. As long as the correct relative

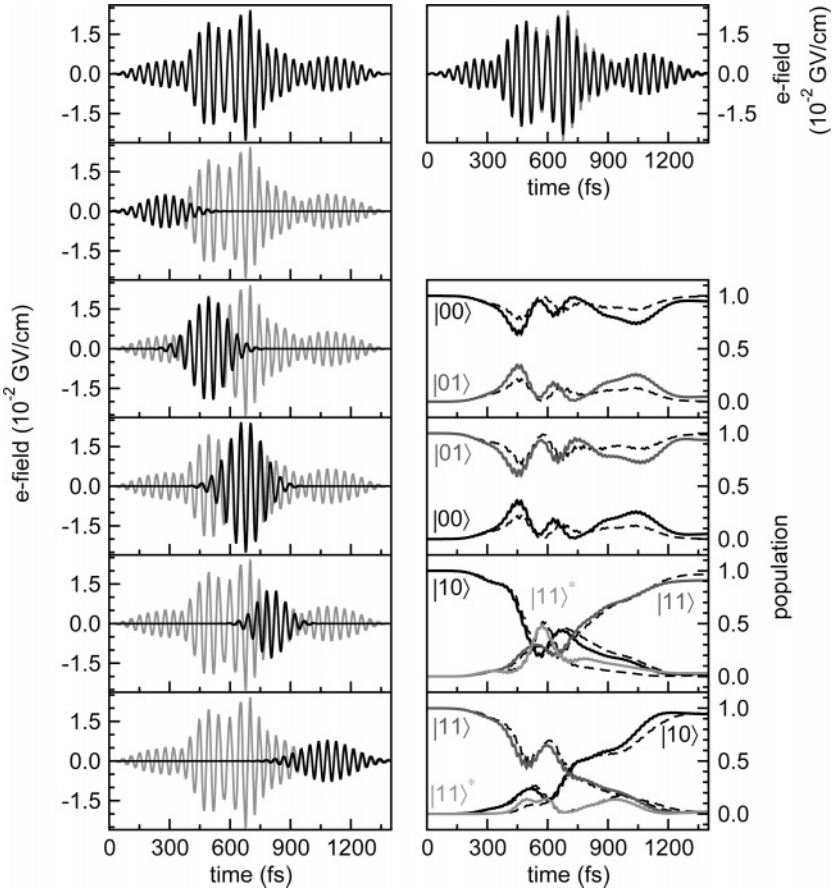

Figure 9. Reconstruction of a CNOT gate in the 3D acetylene model for experimental realization by a train of simply shaped subpulses. Left panels from top to bottom: optimized laser field (black) and the five Gaussian pulses for reconstruction (black) together with the original optimized laser field in gray. Right panels from top to bottom: reconstructed (black) and original (gray) laser fields. The mechanisms of the reconstructed laser fields are indicated by solid lines, and the original mechanisms are indicated by dashed black lines.

phase relation is conserved, a variation of the delay between the subpulses is possible, allowing for some flexibility in the selection of the delay times. This has been demonstrated with simply structured CNOT gates in different two-qubit systems.[39,40] The sensitivity of the pulse sequence to the relative phase is analogous to the dependence of the correct implementation of quantum gate sequences on the relative phase of consecutive elementary gate laser pulses. Figure 9 schematically depicts the reconstruction of a CNOT laser field in a qubit system comprising a state which is anharmonically resonant to the qubit basis state |11⟩, labeled as |11⟩*. The left panels show (from top to bottom) the optimized CNOT laser field and the five Gaussian shaped subpulses as used for its reconstruction, superimposed on the optimized laser field in gray. The right panels show the reconstructed laser field in black superimposed on the originally optimized one in gray. There are only slight deviations in the amplitude profile. The graphs below display the mechanisms of global population transfer induced by the reconstructed CNOT laser pulse sequence together with the original mechanisms, indicated by the dashed lines. Even in this rather complex model system, containing the resonant state |11⟩*, the CNOT gate is reproduced well by the simple Gaussian pulse sequence, with a minimum yield of 91% compared to the 96% of the optimized laser field.

In summary, for all elementary quantum gates in our model systems, a pulse structure could be optimized which is decomposable into a train of simple Gaussian subpulses. Thus, elementary steps of quantum information processing should be realizable in molecular vibrational and/or electronic qubit systems with state-of-the-art (direct and indirect) shaping techniques.

7. Future Challenges

We have reviewed the fundamental concepts of applying molecular systems controlled by femtosecond lasers in quantum information processing, which have been established in theory and experiment. To further promote molecules as practical quantum computing devices in a larger context, work has progressed on issues such as decoherence and scaling.

Control of Decoherence. Theories for the application of optimal coherent control to realize quantum computational operations and algorithms have been established and demonstrated in decoherence-free model systems. Experimental realizations[31−33] of qubit operations have been relying on the fact that qubit logic operations occur on a much shorter time scale than decoherence does. The issue of decoherence is of course an important one for coherent control in general, and research on this topic has been quite extensive (see, e.g., the review by Shapiro and Brumer[72]). In fact, the possibilities inherent in the control of quantum systems by specially shaped laser fields already allow us to counteract a certain amount of dephasing and dissipation, as has been proven, for example, for the case of intramolecular vibrational redistribution, IVR. In the case of IVR, optimal control functionals have been successfully applied to achieve selective state preparation.[59,73,74]

Apart from intramolecular decoherence, also decoherence phenomena which appear through noise from the environ-

ment are important for the practical implementation of quantum computing. Approaches to handle this source of decoherence are mainly concerned with quantum error correction or selection of decoherence-free subspaces.[75] The schemes developed for quantum error correction in general can be straighforwardly transferred to the quantum systems controlled by femtosecond lasers. The error correction scheme, however, requires an even increased scaling of the quantum system with the number of qubits (one logical qubit is encoded in several physical qubits or states) and also in the number of logic operations needed to implement an algorithm (additional error measurement and correction). Within the regime of quantum computing with femtosecond laser fields, two aspects of decoherence control or reduction have been addressed recently: counteracting statistical noise from the environment during quantum logic operations or minimizing noise effects on a desired prepared qubit state. For the first case, fighting decoherence during control or switching processes, Rabitz et al. have actually shown that it is not possible to achieve high yields if the coherence lifetime is short compared to the control interaction time.[76] For the latter case of protection of a prepared quantum or qubit state against noise during free propagation, Kosloff et al. have brought up the idea of a quantum governor, a scheme in which automatical detection and correction of errors without actually measuring the errors is possible.[77]

For practical implementations, we think that it is most useful to fight decoherence by artificially restricting the qubit state space such that decoherence times are much longer than operation times. We have already discussed this approach in the introductory sections on quantum and qubit systems, and it seems quite natural that qubit basis states should be selected that satisfy this precondition. Tannor et al. have additionally brought forth a method of local control which enables the restriction of the evolution of a system to within this selected set of qubit states.[78] Another method of dealing with system internal decoherence is the concept of multilevel encoding. As in quantum error correction, logic qubit states are encoded in multilevel subsystems. However, no readout or error correction steps are necessary, as the quantum logic operations can be constructed in a way that their fidelity is not affected by decoherence within the subsets.[79,80]

Scalability. While, at present, several approaches, headed by ion traps and NMR experiments, but also concepts with photons,[81] solid states,[82] and internal molecular modes,[31,32,33] have demonstrated basic gate operations and are even able to prove that quantum computing has become reality with few qubits,[22−28] large scale quantum computation is still a vision which requires ongoing research. In the end, only a large scale quantum computer will be able to efficiently solve some of the most difficult problems in computational science, such as integer factorization, quantum simulation, and modeling, intractable on any present or conceivable future classical computer.

In principle, two pathways for scaling can be followed: enlargement of a single quantum register, or a network with nodes consisting of smaller units, hopefully achieving both speed and storage capacity increases. The conceptually easiest way to enlarge the qubit system in the molecular approach is to address more normal modes and to use larger molecules. In principle, the number of vibrational qubits in an N-atom molecule scales favorably with $3N$, whereas NMR and ion trap systems scale with N.

In the most advanced NMR and ion trap approaches, the technical difficulties of increasing trap mode densities and increasing gate operation times, arising from the enlargement ansatz, are not yet solved. For molecular vibrational qubits, the challenges are similar. The vibrational spectrum will become more dense, but the high flexibility in molecular design in combination with selection rules can compensate for this difficulty. Up to now, we were able to calculate a four-qubit system (section 4.3) with encouraging results for the gate complexity and efficiency. Still, longer gate operation times were necessary. The estimation of an upper bound for the number of manageable qubits cannot easily be given with theoretical methods, as the limits of computer time will be reached quickly. However, this is not a proof for failure of the direct enlargement ansatz, because in the experiment the molecule will solve its Schrödinger equation on its own and computer time is not an issue. In the ion trap approach, the network type ansatz for enlarging the qubit system seems to be more promising. For molecular qubits, such a scheme could be realized by synthesis of macromolecules consisting of subunits, carbonyl complexes or aromatic ring systems, connected via molecular bridges such as conjugated C−C bonds, allowing parallel distributed computing. Each subunit has to operate as an individual node; thus, the independent control of each node is mandatory. It can again be realized by applying modulated femtosecond pulses, supported by the use of polarization directions. For the communication between the individual nodes, internode information and data exchange is required. Ongoing work in our group shows that it is possible to generate superposition states via molecular wires and thus exchange information between qubits belonging to different nodes. From this point of view the obstacles for the realization of a large scale quantum computer are comparable to those of other technologies under investigation. Aspects in favor of molecules as future building blocks in quantum computing are their special properties which allow convenient handling, storage, fixing, orienting, and precise control by ultrashort laser pulses.

8. Conclusion

In this review, we have discussed the recently developed ideas of using the coherence of internal molecular motion for quantum computing. The appropriate tools to exert coherent control on molecules are shaped, ultrashort, femtosecond to picosecond, laser pulses. They are especially suited for the implementation of quantum information processing, as they provide extremely fast (compared to all other quantum computing implementations), flexible quantum gates, which can act on various degrees of freedom and a manifold of molecular states. Molecules, in turn, provide a wide variety of possible qubit systems, even more when chemical engineering is employed to attain the desired spectroscopic or other characteristics. We have reviewed the possible applications of shaped pulses and molecular qubit systems within two quantum computing approaches: *precompiled* and *universal* quantum computing. The current state of optimal control theory for the calculation of efficient quantum gate laser fields was summarized. Different target definitions have been presented and used for the aspired global population transfer or for phase control. We have elucidated the mechanisms by which logic operations are implemented through laser−molecule interaction for the case of *universal* quantum computing with a set of elementary gates on vibrational qubits. Furthermore, we have outlined

dependencies of the gate complexity on molecular parameters and on the total operation time. We have discussed the role of the phase of the laser field in connection with the relative phase of qubit superposition states in the *universal* approach and the *precompiled* approach. Whether consecutive elementary operations or advanced quantum algorithms are performed, phase stabilization and delicate time synchronization of the applied laser pulses are essential in any case. The appropriate experimental techniques for pulse shaping and, recently, for phase stabilization have been developed and are available for testing in various (quantum computing) control experiments. The ultimate success of femtosecond laser driven molecular qubit systems is not guaranteed, but this approach offers considerable potential as a platform for new ideas and technologies. In this context, optimal control offers the most promising tools to master challenges such as decoherence and scalability.

9. Acknowledgments

The authors thank Brigitte Schneider and Caroline Gollub for valuable contributions and the DFG for financial support through the Schwerpunkt Quantum Information Processing, the Fonds der Chemischen Industrie for continuous financial support, and the EU network CONQUEST.

10. References

(1) May, V.; Kühn, O. *Charge and energy transfer dynamics in molecular systems*; Wiley-VCH: Weinheim, 2005.
(2) Feringa, B. L., Ed. *Molecular switches*; Wiley-VCH: Weinheim, 2003.
(3) Beth, T., Leuchs, G., Eds. *Quantum information processing*, 2nd ed.; Wiley-VCH: Weinheim, 2005.
(4) Tannor, D.; Rice, S. *J. Chem. Phys.* **1985**, *83*, 5013.
(5) Peirce, A. P.; Daleh, M. A.; Rabitz, H. *Phys. Rev. A* **1988**, *37*, 4950. Zhu, W.; Rabitz, H. *J. Chem. Phys.* **1998**, *109*, 385.
(6) Kosloff, R.; Rice, S. A.; Gaspard, G.; Tresigni, S.; Tannor, D. J. *Chem. Phys.* **1989**, *139*, 201.
(7) Judson, R. S.; Rabitz, H. *Phys. Rev. Lett.* **1992**, *68*, 1500.
(8) Assion, A.; Baumert, T.; Brixner, T.; Kiefer, B.; Seyfried, V.; Strehle, M.; Gerber, G. *Science* **1998**, *282*, 919.
(9) Levis, R. J.; Menkir, G. M.; Rabitz, H. *Science* **2001**, *292*, 709.
(10) Brixner, T.; Damrauer, N. H.; Niklaus, P.; Gerber, G. *Nature* **2001**, *414*, 57.
(11) Daniel, C.; Full, J.; González, L.; Lupulescu, C.; Manz, J.; Merli, A.; Vajda, S.; Wöste, L. *Science* **2004**, *24*, 536.
(12) Herek, J. L.; Wohlleben, W.; Cogdell, R. J.; Zeidler, D.; Motzkus, M. *Nature* **2002**, *417*, 533.
(13) Liu, R.-B.; Yao, W.; Sham, L. J. *Phys. Rev. B* **2005**, *72*, 081306.
(14) Spoerl, A. K.; Schulte-Herbrueggen, T.; Glaser, S. J.; Bergholm, V.; Storcz, M. J.; Ferber, J.; Wilhelm, F. K. quant-ph/0504202.
(15) Khaneja, N.; Brockett, R.; Glaser, S. J. *Phys. Rev. A* **2001**, *63*, 032308.
(16) Bouwmeester, D.; Eckert, A.; Zeilinger, A. *The physics of quantum information*; Springer: Berlin, 2000.
(17) Deutsch, D.; Jozsa, R. *Proc. R. Soc. London, A* **1992**, *439*, 553.
(18) Shor P. W. *Proc. 35th Annu. Symp. Found. Comput. Sci.* **1994**, 124.
(19) Grover, L. K. *Proc. 28th Annu. ACM Symp. Theory Comput. (STOC)* **1996**, 212.
(20) DiVincenzo, D. P. *Science* **1995**, *270*, 255.
(21) Brune, M.; Schmidt-Kaler, F.; Maali, A.; Dreyer, J.; Hagley, E.; Raimond, J.; Haroche, S. *Phys. Rev. Lett.* **1996**, *76*, 1800.
(22) Schmidt-Kaler, F.; Häffner, H.; Riebe, M.; Gulde, S.; Lancaster, G. P. T.; Deuschle, T.; Becher, C.; Roos, C. F.; Eschner, J.; Blatt, R. *Nature* **2003**, *422*, 408.
(23) Leibfried, D.; Knill, E.; Seidelin, S.; Britton, J.; Blakestad, R. B.; Chiaverini, J.; Hume, D. B.; Itano, W. M.; Jost, J. D.; Langer, C.; Ozeri, R.; Reichle, R.; Wineland, D. J. *Nature* **2005**, *438*, 639.
(24) Jones, J. A.; Mosca, M. *J. Chem. Phys.* **1998**, *109*, 1648.
(25) Chuang, I. L.; Gershenfeld, N.; Kubinec, M. *Phys. Rev. Lett*. **1998**, *80*, 3408.
(26) Marx, R.; Fahmy, A. F.; Myers, J. M.; Bermel, W.; Glaser, S. J. *Phys. Rev. A* **2000**, *62*, 012310−1.
(27) Vandersypen, L. M. K.; Steffen, M.; Breyter, G.; Yannoni, C. S.; Sherwood, M. H.; Chuang, I. L. *Nature* **2001**, *414*, 883.
(28) Häffner, H.; Hänsel, W.; Roos, C. F.; Benhelm, J.; Chek-al-kar, D.; Chwalla, M.; Körber, T.; Rapol, U. D.; Riebe, M.; Schmidt, P. O.; Becher, C.; Gühne, O.; Dür, W.; Blatt, R. *Nature* **2005**, *438*, 643.
(29) Cirac, J. I.; et al. *Phys. Rev. Lett*. **1997**, *78*, 3221.
(30) Kielpinski, D.; Monroe, C.; Wineland, J. *Nature* **2002**, *417*, 709.
(31) Vala, J.; Amitay, Z.; Zhang, B.; Leone, S. R.; Kosloff, R. *Phys. Rev. A* **2002**, *66*, 062316.
(32) Zadoyan, R.; Kohen, D.; Lidar, D. A.; Apkarian, V. A. *Chem. Phys.* **2001**, *266*, 323.
(33) Bihary, Z.; Glenn, D. R.; Lidar, D. A.; Apkarian V. A. *Chem. Phys. Lett.* **2002**, *360*, 459.
(34) Ohtsuki, Y. *Chem. Phys. Lett*. **2005**, *404*, 126.
(35) Sklarz, S. E.; Tannor, D. J. quant-ph/0404081 (2004).
(36) Tesch, C.; Kurtz, L.; de Vivie-Riedle, R. *Chem. Phys. Lett.* **2001**, *343*, 633.
(37) Tesch, C.; de Vivie-Riedle, R. *Phys. Rev. Lett.* **2002**, *89*, 157901.
(38) Tesch, C.; de Vivie-Riedle, R. *J. Chem. Phys.* **2004**, *121*, 12158.
(39) Troppmann, U.; de Vivie-Riedle, R. *J. Chem. Phys.* **2005**, *122*, 154105.
(40) Korff, B. M. R.; Troppmann, U.; de Vivie-Riedle, R. *J. Chem. Phys*. **2005**, *123*, 244509.
(41) Greenberger, D. M.; Horne, M. A.; Zeilinger, A. *Phys. Today* **1993**, *46*, 22.
(42) Manz, J.; Sundermann, K.; de Vivie-Riedle, R. *Chem. Phys. Lett.* **1998**, *290*, 415.
(43) Kosloff, R. *J. Phys. Chem.* **1988**, *92*, 2087.
(44) Cirac, J. I.; Zoller, P. *Phys. Rev. Lett.* **1995**, *74*, 4091.
(45) Cory, D. G.; Fahmy, A. F.; Havel, T. F. *Proc. Natl. Acad. Sci. U.S.A.* **1997**, *94*, 1634.
(46) Teranishi, Y.; Ohtsuki, Y.; Hosaka, K.; Chiba, H.; Katsuki, H.; Ohmori, K. *J. Chem. Phys.* **2006**, *124*, 114110.
(47) Shapiro, M.; Brumer, P. *J. Chem. Phys.* **1986**, *84*, 4103.
(48) Rice, S. A.; Tannor, D. J.; Kosloff, R. *Faraday Discuss. Chem. Soc*. **1986**, *82*, 2423.
(49) Kuklinski, J. K.; Gaubatz, U.; Hioe, F. T.; Bergmann, K. *Phys. Rev. A* **1989**, *40*, 6741.
(50) Brixner, T.; Krampert, G.; Pfeifer, T.; Selle, R.; Gerber, G.; Wollenhaupt, M.; Graefe, O.; Horn, C.; Liese, D.; Baumert, T. *Phys. Rev. Lett.* **2004**, *92*, 20.
(51) Geppert, D.; Seyfarth, L.; de Vivie-Riedle, R. *Appl. Phys. B* **2004**, *79*, 987.
(52) Abe, M.; Ohtsuki, Y.; Fujimura, Y.; Domcke, W. *J. Chem. Phys.* **2005**, *123*, 1.
(53) Artamonov, M.; Ho, T.-S.; Rabitz, H. *J. Chem. Phys*. **2006**, *124*, 064306.
(54) Assion, A.; Baumert, T.; Bergt, M.; Brixner, T.; Kiefer, B.; Seyfried, V.; Strehle, M.; Gerber, G. *Science* **1998**, *282*, 919.
(55) Hornung, T.; Motzkus, M.; de Vivie-Riedle, R. *J. Chem. Phys*. **2001**, *115*, 3105.
(56) Palao, J. P.; Kosloff, R. *Phys. Rev. A* **2003**, *68*, 062308.
(57) Sundermann, K.; de Vivie-Riedle, R. *J. Chem. Phys.* **1999**, *110*, 1896.
(58) Palao, J. P.; Kosloff, R. *Phys. Rev. Lett.* **2002**, *89*, 188301.
(59) Troppmann, U.; Tesch, C.; de Vivie-Riedle, R. *Chem. Phys. Lett*. **2003**, *378*, 237.
(60) Babikov, D. *J. Chem. Phys.* **2004**, *121*, 7577.
(61) Cheng, T.; Brown, A. *J. Chem. Phys*. **2006**, *124*, 034111.
(62) Gollub, C.; Troppmann, U.; de Vivie-Riedle, R. *New J. Phys*. **2006**, *8*, 48.
(63) Troppmann, U.; Gollub, C.; de Vivie-Riedle, R. *New J. Phys*. **2006**, *8*, 100.
(64) Troppmann, U.; von den Hoff, P.; de Vivie-Riedle, R. In preparation.
(65) Calderbank, A. R.; Shor, P. W. *Phys. Rev A* **1996**, *54*, 1098.
(66) Shor, P. W. quant-ph/9605011, 1996.
(67) Baltuška, A.; Fuji, T.; Kobayashi, T. *Phys. Rev. Lett.* **2002**, *88*, 133901.
(68) Poppe, A.; Holzwarth, R.; Apolonski, A.; Tempea, G.; Spielmann, Ch.; Hänsch, T.; Krausz, F. *Appl. Phys. B* **2001**, *72*, 373.
(69) Witte, T.; Zeidler, D.; Proch, D.; Kompa, K. L.; Motzkus, M. *Opt. Lett.* **2002**, 27, 131.
(70) Tan, H.-S.; Schreiber, E.; Warren, W. S. *Opt. Lett.* **2002**, *27*, 439.
(71) Shim, S.-H.; Strasfeld, D. B.; Fulmer, E. C.; Zanni, M. T. *Opt. Lett*. **2005**, *31*, 838.
(72) Shapiro, M.; Brumer, P. *Phys. Rev*. **2006**, *425*, 195.
(73) Goswami, D. *Phys. Rev. Lett*. **2002**, *88*, 177901.
(74) Witte, T. T.; Hornung, T.; Windhorn, L.; Proch, D.; de Vivie-Riedle, R.; Motzkus, M.; Kompa, K.-L. *J. Chem. Phys*. **2003**, *118*, 2021.
(75) Nielsen, M. A.; Chuang, I. *Quantum Computation and Quantum Information*; Cambridge University Press: 2000.
(76) Shuang, F.; Rabitz, H. *J. Chem. Phys*. **2006**, *124*, 154105.
(77) Kallush, S.; Kosloff, R. *Phys. Rev. A* **2006**, *73*, 032324.

(78) Sklarz, S. E.; Tannor, D. J. *Chem. Phys*. **2006**, *322*, 87.
(79) Grace, M.; Brif, C.; Rabitz, H.; Walmsley, I.; Kosut, R.; Lidar, D. *New J. Phys.* **2006**, *8*, 35.
(80) Grace, M.; Brif, C.; Rabitz, H.; Walmsley, I.; Kosut, R.; Lidar, D. *J. Phys. B* **2007**, *40*, 103.
(81) Knill, E.; Laflamme, R.; Milburn, G. *Nature* **2001**, *409*, 46.
(82) Koch, R. H.; Keefe, G. A.; Milliken, F. P.; Rozen, J. R.; Tsuei, C. C.; Kirtley, J. R.; DiVincenzo, D. P. *Phys. Rev. Lett.* **2006**, *96*, 127001.

CR040094L